ANALYSIS OF REINFORCED CONCRETE BEAMS WITH FERROCEMENT OVERLAY

MAHBUBA BEGUM

DEPARTMENT OF CIVIL ENGINEERING
BANGLADESH UNIVERSITY OF ENGINEERING AND TECHNOLOGY

DECEMBER, 2001

ANALYSIS OF REINFORCED CONCRETE BEAMS WITH FERROCEMENT OVERLAY

By

Mahbuba Begum

A Thesis Submitted in Partial Fulfillment for the
Requirements of the Degree of
Master of Science in Civil Engineering

Department of Civil Engineering,
Bangladesh University of Engineering and Technology, Dhaka

December, 2001

ANALYSIS OF REINFORCED CONCRETE BEAMS WITH FERROCEMENT OVERLAY

A THESIS BY

MAHBUBA BEGUM

Approved as to the style and content by

Dr.Ahsanul Kabir
Professor
Department of Civil Engineering
BUET, Dhaka - 1000.

Chairman
(Supervisor)

Dr. Md. Abdur Rouf
Professor and Head
Department of Civil Engineering
BUET, Dhaka - 1000.

Member

Dr. M. Shamim Z. Bosunia
Professor
Department of Civil Engineering
BUET, Dhaka - 1000.

Member

Dr. Sk. Sekender Ali
Professor
Department of Civil Engineering
BUET, Dhaka - 1000.

Member

Engr. Akhtaruzzaman
M.Sc. Engg.(AIT), GMIE,UK
Managing Director
Texture Consultants
3/8, Lalmatia, Block-F, Dhaka.

Member
(External)

Declaration

Except for the contents where specific reference have been made to the work of others, the studies embodied in this thesis is the result of investigation carried out by the author. No part of this thesis has been submitted to any other University or other educational establishment for a Degree, Diploma or other qualification (except for publication).

Mahbuba Begum 24/12/01

Author

ACKNOWLEDGEMENT

The work described in this thesis was carried out under the supervision of Dr. Ahsanul Kabir, Professor of Civil Engineering Department, Bangladesh University of Engineering and Technology, Dhaka. The author wishes to express her indebtedness and gratitude to him for his constant supervision, continuous guidance, helpful criticism, invaluable suggestions and unfailing encouragement given throughout the course of this work.

The author expresses her gratefulness to the Head, Department of Civil Engineering, BUET for providing all the laboratory and computation facilities to materialize this work. The author acknowledges with gratitude the valuable suggestions of Dr. Sk. Sekender Ali, Professor of Civil Engineering, Bangladesh University of Engineering and Technology at different stages of this research work. The author is grateful to Dr. K.M. Amanat, Associate Professor of Civil Engineering for his suggestions and help regarding finite element modeling in ANSYS.

The author acknowledges the co-operation and help of the members of staff of Civil Engineering Department, BUET. Above all, the author expresses her gratitude to Allah (SWT) to whom belongs ALL GLORY, WHO has wished this work to bring to reality.

Mahbuba Begum

ABSTRACT

Serviceability of a concrete structure is determined by its deflection, cracking, extent of corrosion of its embedded reinforcement and surface deterioration. A satisfactory performance of reinforced concrete structures over their design life under a combination of various types of loads requires a crack free structure so as to prevent ingress of moisture by diffusion. This ultimately leads to corrosion of steel, carbonation of concrete and leaching of soluble soft lime products. Thus, the life and strength of the structure is reduced. Serviceability of the structure can be greatly improved providing a low permeable cover such as ferrocement overlay to the reinforced concrete elements. If this cover can be used as formwork for the structural elements it may significantly reduce the cost of timber shuttering and formwork for those elements.

An attempt has been made in this research to study the behavior of reinforced concrete beams with ferrocement overlay. An analytical model has been developed based on the basic assumptions of reinforced concrete and on the idealized stress-strain diagrams of the constituent materials. A linear elastic finite element study was also carried out to observe the serviceability of such beams. The performance of both the analytical and the layered finite element model for the composite beam is validated by comparing these results with some existing experimental results. The proposed analytical model is found to perform quite well within the serviceability limit and fair enough at the ultimate limit state.

The analytical method proposed is used to calculate the load-displacement response for three sets of beams with varying ferrocement properties. The serviceability of the beams is found to be significantly improved by increasing the number of mesh layers for a constant ferrocement thickness. The confinement effect of the ferrocement overlay on the concrete core is also investigated using the finite element model. The resulting flexural stresses in the concrete core were found to be significantly improved compared to its unconfined state under identical loading condition. Obviously, ferrocement overlay improves the ductility of the RC beams which is very important for the structures in seismic regions. The inherent crack arresting capacity of ferrocement is expected to enhance the life of concrete beams and hence the durability.

CONTENTS

Chapter 1

INTRODUCTION

1.1 General

In recent years repair and rehabilitation of the existing structures has become one of the most challenging problem in Civil Engineering. Defects, failure and general distress in the structures could be the result of structural deficiency caused by erroneous design, poor workmanship or overloading of the structure. It could also be caused by corrosion, fire and natural disasters. A damaged or distressed structure can be repaired or renovated to a satisfactory level of performance at a reasonable cost by different methods. One of the cheapest and most widely used methods of strengthening is the use of ferrocement coatings in the distressed element.

From several investigations it has been found that ferrocement is an ideal material for rehabilitation and restrengthening of structures because it improves crack resistance combined with high toughness, the ability to be cast into any shape, rapid construction with no heavy machinery, small additional weight imposed and low cost of construction [Pama,1994]. In Bangladesh ferrocement material has been used extensively in repairing and strengthening of distressed structural elements of the buildings. This versatile material has enormous potentials as a protective cover of the structural elements against corrosion in the coastal areas of the country. It is well known that in Bangladesh conventional formwork normally contributes 20% to 25% of the cost of reinforced concrete. Significant economic advantages may occur if the ferrocement cover can be used as permanent formwork for reinforced concrete beams. In addition, structural benefits may be obtained if the ferrocement layer can be made to act compositely with the concrete core of the member.

Ferrocement is a type of thin-wall reinforced concrete commonly constructed of hydraulic cement mortar, reinforced with closely spaced layers of continuous and relatively small diameter wire mesh. It is considered to be an extension of reinforced

concrete technology with relatively better mechanical properties and durability than ordinary reinforced concrete. Within certain loading limits, it behaves as a homogenous elastic material and these limits are wider than for normal concrete. The uniform distribution and high surface area to volume ratio of its reinforcement results in better crack arrest mechanism, i.e. the propagation of cracks are arrested resulting in high tensile strength of the materials [Pama and Paul,1978, ACI Committee 549,1993]. Due to this high resistance to crack, ferrocement can be used as a low permeability cover layer for reinforced concrete. This protective layer may be precast and can be used as permanent formwork to the concrete element. With the increasing cost of timber and shuttering the use of ferrocement as permanent formwork look's like an economically viable alternative. Ferrocement as permanent formwork can not only replace the conventional timber and steel shuttering but also improves the serviceability of the structural element through better crack resistance and less deterioration of reinforcement due to corrosion in aggressive environment.

Already several experimental investigations have been carried out to observe the structural effectiveness of ferrocement as permanent formwork for reinforced concrete elements. May's et.al.,1994, reported that the increase in strength of 15% over conventional reinforced concrete elements was achieved by the use of permanent ferrocement formwork. Kadir et.al., 1997, also found that the ferrocement formwork for reinforced concrete beams with and without shear connectors contributed about 21%-75% and 16%-50% to the flexural strength respectively. The behavior of ferrocement reinforced concrete composite beams have also been studied in the serviceability and ultimate limit states by Rosenthal and Bljuger,1985. Cracking moments of the composite beams were found to be 11% and 13% higher than those of the reference reinforced concrete beams, due to the additional tensile strength contributed by the ferrocement cover. It was also observed that cracks in the composite beams had only reached, at failure, a width of 0.4 mm to 0.5 mm, as compared to twice as much in the reference beams.

Most of the research works regarding ferrocement reinforced concrete beams were limited to the evaluation of the superior performance of these beams as compared to the ordinary reinforced concrete beams. But the composite behavior of ferrocement

with reinforced concrete was not fully investigated and there is no definite guideline for the design and analysis of ferrocement reinforced concrete beams. A significant number of experiments have been carried out but the effort on formulating a rational basis for analytical investigations has been lacking. This research may be considered as an attempt to that end. An analytical study on the behavior of the reinforced concrete beams with ferrocement overlay has been carried out here to provide a simple and direct analytical procedure for such beams.

1.2 Ferrocement - An Overview

Ferrocement is a highly versatile form of reinforced concrete, constructed of hydraulic cement mortar reinforced with closely spaced layers of continuous and relatively small diameter wire mesh. The mesh may be made of a metallic or other suitable material. Ferrocement primarily differs from conventional reinforced or prestressed concrete by the manner in which the reinforcing elements are dispersed and arranged. In this regard In this regard The American Concrete Institute (ACI) Committee 549 put forward the definition of ferrocement as follows:

"Ferrocement is a type of thin wall reinforced concrete construction where usually a hydraulic cement is reinforced with layers of continuous and relatively small diameter mesh. Mesh may be made of metallic material or other suitable materials."

Ferrocement has gained widespread popularity in the developing nations. It has certain inherent advantages and has been accepted as a suitable technology for developing countries for the following reasons:

(a) Its basic raw materials are readily available in most countries.
(b) It can be fabricated into any desired shape.
(c) The skills for ferrocement construction can be acquired easily.
(d) Heavy plants and machinery are not involved in ferrocement construction.
(e) In case of damage, it can be repaired easily.
(f) Being labor intensive, it is relatively inexpensive in developing countries.

1.3 Objective of the Present Study

The objectives of the present study are,

(i) To study the behavior of a reinforced concrete beam with ferrocement overlay and to present a direct and simple analytical method for the analysis of such beams.

(ii) To perform a linear elastic finite element analysis of the composite behavior of the ferrocement coated reinforced concrete beam in order to determine the load/ moment that causes the first crack to appear and compute the corresponding deflection.

(iii)To study the confinement effect of ferrocement overlay on the concrete core with the help of the finite element modeling.

(iv)To verify the analytical method developed here with some existing experimental results and with the finite element analysis using ANSYS as well.

(v) To investigate the influence of various parameters on the load-deflection response of the composite beams and finally to provide some suggestions for the design of such beams.

1.4 Scope of the Study

The present research has been undertaken to study the behavior of reinforced concrete beams with ferrocement overlay using two different approaches. To study this effect, a simple analytical formulation is developed and a rigorous finite element analysis (using a package software) has been carried out. The latter method is also used to validate the simple formulation proposed. The salient features within the scope may be summarized as follows.

(i) A simple analytical method based on the basic principles of reinforced concrete is adopted for the analysis of ferrocement reinforced composite beams under flexure. The method considers the effect of the horizontal ferrocement layer at the bottom of the reinforced concrete beam for flexural analysis. Effect of the shear forces on the flexural behavior has not been considered in this analysis.

(ii) The analytical formulation idealizes the nonlinear response of the ferrocement reinforced concrete beam under monotonically increasing load as a trilinear load-deflection curve and the analysis can proceed through the three distinct stages.

(iii) The finite element package, ANSYS has been used to predict the elastic behavior upto cracking. Layered solid element is used for finite element modeling to observe the efficiency of this layered modeling for the composite section. The layers can allow material variations and can accommodate composite materials. Complete modeling of the composite section including the concrete core and both the vertical and horizontal ferrocement layers are modeled using layered solid elements.

(iv) A reinforced concrete beam without ferrocement overlay is also modeled with layered solid finite elements to determine the confinement effect of ferrocement layer on the basic concrete beam.

(v) The effect of the number of mesh layers and thickness of the ferrocement cover on the cracking and ultimate behaviour of the beam has been studied using the simple analytical model. The finite element model has been employed to assess the effect of these parameters on the confinement of ferrocement cover.

Chapter 2

LITERATURE REVIEW

2.1 Introduction

To study the effect of ferrocement overlay on reinforced concrete elements, first it is necessary to study the behavior of ferrocement under different conditions. In this regard it is necessary to identify the parameters affecting the properties of ferrocement and review relevant literature in this field. This chapter presents a brief literature review on the properties of ferrocement and concrete relevant to this study. Experimental investigations carried out by several researchers on the behavior of a reinforced concrete beam with ferrocement overlay are also included.

2.2 Properties of Ferrocement

Ferrocement, considered to be an extension of reinforced concrete technology, has relatively better mechanical properties and durability than ordinary reinforced concrete. Within certain loading limits, it behaves as a homogenous elastic material and these limits are wider than for normal concrete. The uniform distribution and high surface area to volume ratio of its reinforcement results in better crack arrest mechanism, i.e. the propagation of cracks are arrested resulting in high tensile strength of the materials [Pama, 1990].

Many of the properties unique to ferrocement derive from the relatively large amount of two-way reinforcement made up of relatively small elements with much higher surface area than conventional reinforcement. In the words of Nervi, who first used the term ferrocement, its most notable characteristic is "greater elasticity and resistance to cracking given to the cement mortar by the extreme subdivision and distribution of the reinforcement". Therefore, the recognition of parameters defining the subdivision and distribution of the reinforcement is fundamental in understanding many of the properties of ferrocement.

2.2.1 Reinforcing Mesh

One of the essential components of ferrocement is wire mesh. Different types of wire meshes are available almost everywhere. Common wire meshes have hexagonal or square opening. Meshes with hexagonal openings are sometimes referred to as chicken wire mesh or aviary mesh. They are not structurally as efficient as meshes with square opening because the wires are not always oriented in the directions of the principal (maximum) stresses. However, they are very flexible and can be used in doubly curved elements.

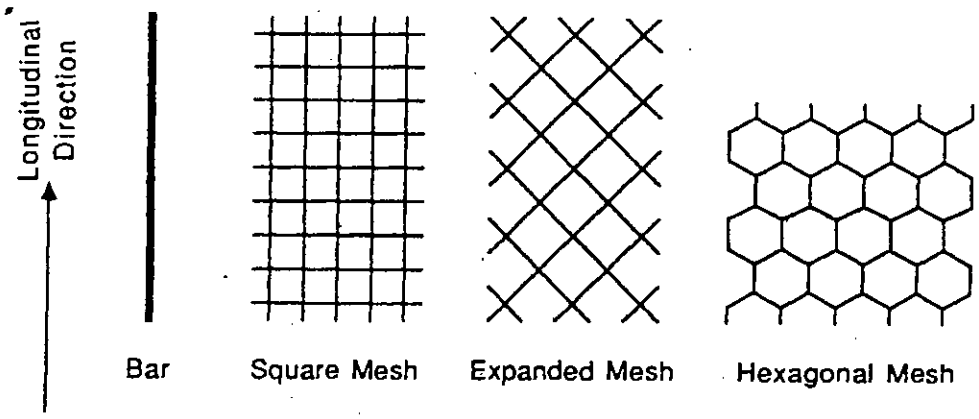

Fig.2.1: Different Types of Mesh used in Ferrocement (ACI Committee 549, 1993)

Meshes with square opening are available in welded or woven form. Welded-wire mesh is made of straight wires in both the longitudinal and transverse directions. Thus welded-mesh thickness is equal to two wire diameters. Woven mesh is made of longitudinal wires woven around straight transverse wires. Depending on the tightness of the weave, woven-mesh thickness may be up to three wire diameters. Welded-wire meshes have a higher modulus and hence higher stiffness than woven meshes; they lead to smaller crack widths in the initial portion of the load-deformation curve. Woven-wire meshes are more flexible and easier to work with than welded meshes. However, welding anneals the wire and reduces its tensile strength [ACI Committee 549, 1993].

Three parameters are commonly used in characterizing the reinforcement in ferrocement applications: the volume fraction, the specific surface of reinforcement, and the effective modulus of the reinforcement. These are discussed below.

2.2.1.1 Volume Fraction of Reinforcement

Volume fraction (V_f) is the total volume of reinforcement divided by the volume of composite (reinforcement and matrix). For a composite reinforced with meshes with square openings, V_f is equally divided into V_{fl} and V_{ft} for the longitudinal and transverse directions, respectively. For other types of reinforcement V_{fl} and V_{ft} may be unequal. For ferrocement reinforced with square or rectangular mesh, the volume fraction of mesh reinforcement can be calculated from the following relation,

$$V_f = \frac{N\pi d_b^2}{4h}\left(\frac{1}{D_l} + \frac{1}{D_t}\right) \tag{2.1}$$

where, N=number of layers of mesh reinforcement

d_b = diameter of mesh wire

h = thickness of ferrocement

D_l = center-to-center spacing of wires aligned longitudinally in reinforcing mesh

D_t = center-to-center spacing of wires aligned transversely in reinforcing mesh

2.2.1.2 Specific Surface of Reinforcement

Specific surface, S_r is the total bonded area of reinforcement (interface area or area of the steel that comes in contact with the mortar) divided by the volume of composite. S_r is not to be confused with the surface area of reinforcement divided by the volume of reinforcement. For a composite using square meshes, S_r is divided equally into S_{rl} and S_{rt} in the longitudinal and transverse directions, respectively.

For a ferrocement plate of width b and depth h, the specific surface of reinforcement can be computed from:

$$S_r = \frac{\sum_0}{bh} \tag{2.2.a}$$

in which $\sum_0$ is the total surface area of bonded reinforcement per unit length.
For square or rectangular mesh the expression for S_r will become,

$$S_r = \frac{\pi\, d_b (D_l + D_t)}{D_l . D_t . h} \tag{2.2.b}$$

Relation between S_r and V_f

The relation between S_r and V_f when square-grid wire meshes are used is,

$$S_r = \frac{4V_f}{d_b} \tag{2.3}$$

where d_b is the diameter of the wire. For other types of wire meshes, S_{rl} and S_{rt} may be unequal.

2.2.1.3 Effective Modulus of the Reinforcement

Although most ferrocement properties have similar definition as those of reinforced concrete, one property is defined differently. It is the effective modulus of the reinforcing system E_r. This is because the elastic modulus of a mesh (steel or other) is not necessarily the same as the elastic modulus of the filament (wire or other) from which it is made. In a woven steel mesh, weaving imparts an undulating profile to the wires. When tested in tension, the woven mesh made from these wires stretches more than a similar welded mesh made from identical straight wires. Hence, the woven mesh behaves as if it has a lower elastic modulus than that of the steel wires from which it is made. Design values for common meshes used in ferrocement construction are recommended in Table 3.1.

Table 2.1 Minimum values of yield strength and effective modulus for steel meshes and bars recommended for design [ACI Committee 549, 1993]

		Woven square mesh	Welded square mesh	Hexagonal mesh	Expanded metal mesh	Longitudinal bars
Yield strength	F_y, ksi (Mpa)	65 (450)	65 (450)	45 (310)	45 (310)	60 (414)
Effective modulus	$(E_r)_{long}$ 10^3 ksi (10^3 Mpa)	20 (138)	29 (200)	15 (104)	20 (138)	29 (200)
	$(E_r)_{trans}$ 10^3 ksi (10^3 Mpa)	24 (165)	29 (200)	10 (69)	10 (69)	—

2.2.1.4 Effective Area of Reinforcement

The area of reinforcement per layer of mesh considered effective to resist tensile stresses in a cracked ferrocement section can be determined as follows,

$$A_{si} = \eta V_{fi} A_c \tag{2.4}$$

where, A_{si} = effective area of reinforcement for mesh layer i

η = global efficiency factor of mesh reinforcement in the loading direction considered.

V_{fi} = volume fraction of reinforcement for mesh layer i

A_c = gross cross sectional area of mortar (concrete) section.

Table 2.2 Recommended Design Values of the Global Efficiency Factor η of Reinforcement for a Member in Uniaxial Tension or Bending (ACI Committee 549,1993)

		Woven square mesh	Welded square mesh	Hexagonal mesh	Expanded metal mesh	Longitudinal bars
Global efficiency factor	Longitudinal η_l	0.50	0.50	0.45	0.65	1
	Transverse η_t	0.50	0.50	0.30	0.20	0
	At 45 deg. $\eta\theta=45$	0.35	0.35	0.30	0.30	0.70

The global efficiency factor when multiplied by the volume fraction of reinforcement, gives the equivalent volume fraction (or equivalent reinforcement ratio) in the loading direction considered. In effect, it leads to an equivalent (effective) area of reinforcement per layer of mesh in that loading direction. For square mesh, is equal to 0.5 when loading is applied in one of the principal directions. For a reinforcing bar loaded along its axis. η=1).

2.2.2 Ferrocement in Tension

The tensile characteristics of ferrocement have not yet been fully defined and standardized. In tension, the load-carrying capacity is essentially independent of specimen thickness because the matrix cracks well before failure and does not - contribute directly to composite strength. The influence of types, sizes and volumes of wire meshes on elastic cracking and ultimate behavior of ferrocement in uniaxial tension have been studied by Naaman and Shah, 1971. They observed that the ultimate tensile strength of ferrocement is the same as that of the mesh alone. The specific surface of the reinforcement strongly influences the cracking behavior of ferrocement. Some technical information have been released [Lee et.al., 1972, Nanni and Zollo,1987], but their results seem to be specific to certain types of mesh reinforcement. For square mesh reinforcements, the load-elongation behavior of ferrocement in tension has been characterised in three stages [Naaman and Shah,1971; Pama et.al.,1974]. In the initial stage, the matrix and reinforcement act as a continuum having a composite elastic modulus approximately equal to that predicted from the volumetric law of mixtures of the longitudinal reinforcement and the matrix. Naaman and Shah have shown that a safe lower bound value of composite modulus of elasticity can be predicted by assuming the volume of mortar unity. Thus, the modulus of elasticity of ferrocement for uncracked state is determined as,

$$E_f = E_m(1-V_l) + E_{fs}V_l \cong E_m + E_{fs}V_l \qquad (2.5)$$

where, E_m=Modulus of elasticity of mortar

E_{fs} =Modulus of elasticity of wire mesh

V_l =Volume fraction in the loading direction

The second stage of the load-deformation behavior, associated with a fully cracked matrix, is also linear. Its modulus is somewhat greater than the product of the volume fraction and the modulus of the longitudianl reinforcement. The mortar and the lateral reinforcement continue to play an active role after first cracking, either individually or in combination [Naaman and Shah,1971; Pama et.al.,1974]. In the third stage, the matrix ceases to play a role and failure corresponds to the yielding of the reinforcement.

2.2.3 Ferrocement in Compression

In this mode, unlike tension, the matrix contributes directly to ferrocement strength in proportion to its cross-sectional area. Compressive strength of ferrocement (regardless of the amount of mesh reinforcement) seems to be much the same as that of mortar alone [Rao,1969]. The experimental results showed that under compression the ultimate compressive strength is lower than that of equivalent pure mortar [Pama et.al.,1974]. The compressive strength at ultimate condition is assumed to be $0.85f_c'$ where f_c' is the ultimate compressive strength of the mortar. An investigation into the behavior of ferrocement specimen in direct compression has been discussed by Rao. Conclusions were drawn with respect to the effect, of percentage of reinforcement and the size of reinforcement on the behavior of ferrocement. Smaller diameter wire mesh would be preferable to use as this gives higher elasticity and higher ultimate compressive strengths for the same percentage of reinforcement, all the other factors remaining essentially the same. When mesh reinforcement is arranged parallel to the applied load in one plane only, no improvement in strength is observed [Pama, et. al.,1974]. The only forms of reinforcement likely to result in significant strength gains in compression are square mesh reinforcements [ACI Committee Report 549, 1993] fabricated in closed box or cylindrical arrangements which restrain the matrix, thus forcing it to adopt a triaxial stress condition with associated higher strength.

2.2.4 First Cracking Strength of Ferrocement

The term first-crack strength or its equivalent appears frequently in literature on the behavior of ferrocement under tension and flexure, but its use without qualification is unfortunate because it can be defined in various ways and therefore can mean different things to different people. In a comprehensive discussion of this problem [Walkus, 1975], it is noted that microcracks are inherent in the mortar matrix even before it is loaded, and that as the microcracks widen, propagate, and progressively join together under load, they are detected by some means, visual or otherwise, and termed "first cracks." However, in the various Polish and Russian studies [Walkus,1975], "first cracking" is defined by a crack width ranging from 2×10^{-4} in. (0.005 mm) to a value visible to the naked eye,' $1.2\text{-}3.3 \times 10^{-3}$ in. (0.03-0.1 mm). In other studies, first-cracking is defined as the first deviation from linearity of the load-elongation function in tension (900-1500 microstrain) or the corresponding deviation of the load-deflection curve in flexure (Balaguru et.al.,1977), also as a crack width under flexural loading of 0.003 in.(0.075 mm); as the point at which the matrix at the tension face of flexural specimen reaches a strain equal to the cracking strain of the unreinforced matrix, or simply as the first visible crack [Johnston et.al.,1974]. Therefor, it is necessary to perform experimental investigations for accurate prediction of the first cracking stress of ferrocement in direct tension and in flexure.

Research studies have shown that crack width in reinforced concrete structures can be reduced by increasing the bond between the reinforcement and the concrete, by increasing the distribution of the reinforcement and by reducing the thickness of the cover. All these factors are favorable for ferrocement. Crack width is nearly zero at the interface between the steel and the mortar and increases from the interface towards the surface. Therefore, the smaller the distance between the interface and the surface of the structure, i.e., the cover, the smaller the crack width. Specific surface and volume fraction of the reinforcement are found to play a significant role in the cracking behavior of ferrocement and their influences are studied by several researchers and empirical relation ships between these parameters and the first cracking stress are proposed.

Experimental evidence from the work of Surya Kumar and Sharma (1976) showed that the first crack stress in bending is a linear function of the percentage of steel reinforcement and they suggested an empirical relation,

$$f_{rf} = 284p + 483 \qquad psi$$
$$f_{rf} = 1.96p + 3.33 \qquad MPa \tag{2.6}$$

where, p = percentage of reinforcement by volume or the volume fraction of the reinforcing mesh.

On the other hand Logan and Shah (1973) showed that the first crack stress in bending is a linear function of the specific surface and they presented an empirical equation relating these two parameters as follows:

$$f_{rf} = 1600S_{rl} + f_m \qquad psi$$
$$f_{rf} = 280.20S_{rl} + f_m \qquad MPa \tag{2.7}$$

Where, S_{rl} = the specific surface of the reinforcement in loading direction and f_m=modulus of rupture of plain mortar

2.3 Stress-Strain Behavior of Concrete

Knowledge of the stress-strain relationship of concrete is essential for developing analysis and design procedures for concrete structures. Fig.2.2 shows a typical stress-strain curve obtained from tests using cylindrical concrete specimens loaded in uniaxial compression over several minutes. The first portion of the curve, to about 40% of the ultimate strength f_c', can essentially be considered linear for all practical purposes. Beyond approximately 70% of the ultimate strength, the material loses its stiffness significantly, thereby increasing the curvilinearity of the diagram [Nawy,1990]. In this study the concrete stress-strain curve is assumed as a parabolic form (Fig.2.2(c)) following Hognestad [Lin and Burns, 1982] very closely. This is convenient because it allows integration to solve the resultant compressive force, and its location in a closed form solution as shown in Fig.2.2.

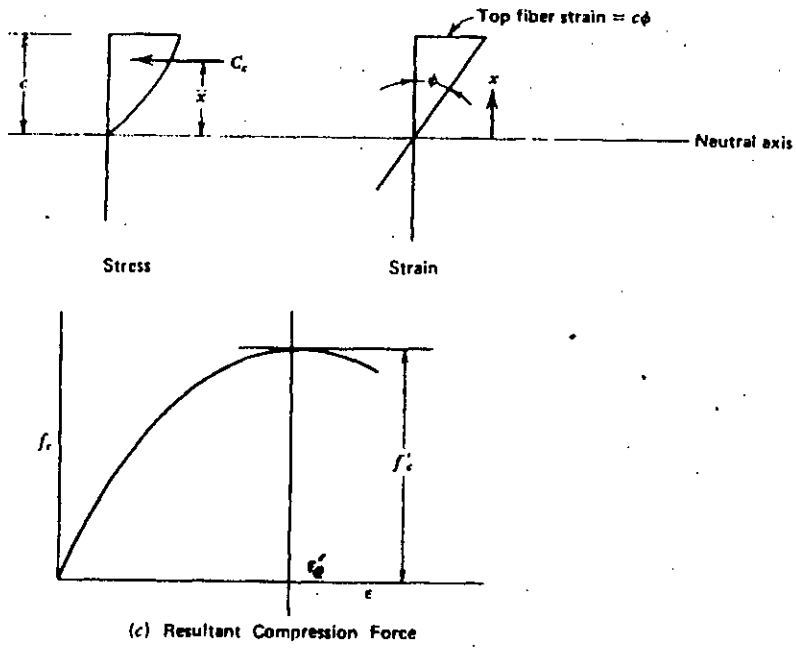

Fig.2.2 Stress-Strain Properties for Concrete

Concrete stress = $f_c = f_c'\left[\frac{2\phi x}{c} - \left(\frac{\phi x}{c}\right)^2\right]$ as shown in Fig.2.2

where $\phi x = \varepsilon$ in the expression from Hognestad similar to 2.2(c)

$$C_c = \int_0^c f_c b dx = b f_c' \int_0^c \left(\frac{2\phi x}{\varepsilon_c'} - \frac{\phi^2 x^2}{\varepsilon_c'}\right) dx$$

solving this, the resultant compression force for a rectangular section is,

$$C_c = b f_c' \frac{\phi}{\varepsilon_c'} c^2 \left[1 - \frac{\phi c}{3\varepsilon_c'}\right] \tag{2.8}$$

$\bar{x} C_c = \int_0^c (f_c b dx) x$ substituting the expression above for C_c and rearranging terms, the distance from neutral axis to line of action for resultant compression force is,

$$\bar{x} = c\left[\frac{8\varepsilon_c' + 3\phi c}{12\varepsilon_c' - 4\phi c}\right] \tag{2.9}$$

Here the value of strain ε_c', corresponding to the ultimate stress f_c' can be calculated from the following expression [Collins and Mitchell, 1991].

$$\varepsilon_c' = \frac{f_c'}{E_c} \frac{n}{n-1} \tag{2.10}$$

where, n is the curve-fitting factor equal to $E_c/(E_c-E_c')$ and E_c and E_c' are the initial and ultimate secant modulus respectively for concrete.

A suitable expression for n for normal-weight concrete is,

$$n = 0.8 + \frac{f_c'}{2500} \qquad psi$$
$$n = 0.8 + \frac{f_c'}{17} \qquad MPa \tag{2.11}$$

The secant modulus of elasticity E_c for normal-weight concrete is estimated from the following expression given in ACI Code.

$$E_c = 57{,}000\sqrt{f_c'} \qquad psi$$
$$E_c = 4730\sqrt{f_c'} \qquad MPa \tag{2.12}$$

Calculated values of E_c, ε_c' and n using the above equations for different strength values of normal-weight concrete are given in Table 2.3.

Table2.3Compressive Stress-strain Coefficients for Normal-weight Concrete(Collins and Mitchell,1991)

f_c'	psi (Mpa)	3000 (20.7)	3500 (24.1)	4000 (27.6)	5000 (34.5)	6000 (41.4)	8000 (55.2)	10,000 (69.0)	12,000 (82.7)
E_c	ksi (Mpa)	3191 (22000)	3366 (23200)	3530 (24300)	3828 (26400)	4098 (28300)	4578 (31600)	5000 (34500)	6060 (41800)
$\epsilon_c' \times 1000$		1.88	1.91	1.94	2.03	2.13	2.33	2.53	2.71
n		2.00	2.20	2.40	2.80	3.20	4.00	4.80	5.60

2.4 Experimental Investigations on Ferrocement Reinforced Concrete Beams

Research and development work on ferrocement has progressed at a tremendous pace during recent years and a variety of structures using innovative design and construction techniques have been built worldwide. As a result, a large volume of

technical information is now available on various aspects of ferrocement design, construction, maintenance and repair. Increasing popularity and growing public acceptance have made it necessary to formulate design guidelines by collating the available information. Efforts have also been made in recent years to improve the performance of reinforced concrete elements by applying ferrocement overlay. The concept has been intuitively applied for repair and restrengthing of distressed elements.

Anwar et. al. investigated the rehabilitation technique for reinforced concrete structural beam elements using ferrocement. The technique involved strengthening of the reinforced concrete beams by application of hexagonal chicken wire mesh and skeletal steel combined by ordinary plastering. Lub and van Wanroji strengthened existing beams in reinforced concrete building structures by means of shotcrete-ferrocement. It was found that the mesh is fully effective and a monolithic condition of the shotcrete layer and original concrete beam is attained. The wire mesh was found to act as excellent shear force reinforcement.

Rosenthal and Bljuger studied the flexural behaviour of ferocement-reinforced concrete composite beams in the serviceability and ultimate limit states. The flexural behaviour of four rectangular composite beams made of low-strength concrete, and encased in thin skin elements made of high-strength ferrocement, was compared with four reference beams in the serviceability and ultimate limit states. In doing so, special deformational and crack-formation properties of the encasing elements (reinforced with wire meshes) were exploited, resulting in hair cracks which appear in the beams under service load, rather than regular width cracks. Cracking moments of the composite beams were 11% and 13% higher than those of the reference beams, due to the additional flexural tensile strength contributed by the skin elements. Cracks in the composite beams have only reached, at failure, a width of 0.4 mm to 0.5 mm, as compared to twice as much in the reference beams. Composite action between the skin and core components was fully obtained until crack appearance. Beyond that stage and upto failure, a partial separation might have happened, according to somewhat different crack patterns of the reference and composite beams.

In 1994, G.C. Mays and Barnes reported the results of structural effectiveness of ferrocement as permanent formwork to reinforced concrete elements. From this investigation they found that the increase in strength of 15% over conventional reinforced concrete elements was achieved by the use of permanent ferrocement formwork and it was also observed that ferrocement is a potentially durable material in aggressive environments. It has superior crack control to conventional reinforced concrete and can be successfully combined with other material to form composites.

Kaushik and Dubey studied the performance of R.C. ferrocement composite beams through experimental investigation on RC beam cast on ferrocement and distressed beam rehabilitated by ferrocement jacketing. They reported that the increase in ultimate strength compared to RC beams was 44% for composite beams and 39% for rehabilitated beams. This shows that composite beams and rehabilitated beams are capable of performing equally well. Moreover, the ultimate strength and stiffness of R.C. beam can be significantly increased by strengthening with precast ferrocement plates in the shear failure zone . Therefore, ferrocement can satisfactorily be used as the precast part of the composite in which R.C. beam is cast.

An experimental investigation was carried by Kadir et. al., 1997 to study the ultimate load, flexural behavior and mode of failure at collapse of reinforced concrete beams using ferrocement permanent formwork (composite beam). The linkage between the two materials was achieved by placing shear connectors along the length of the beam. Test results showed that the reinforced concrete beams with ferrocement permanent formwork failed by flexure. The composite beam with shear connectors carried about 12% higher load and 10% reserved flexural strength and showed lower deflection when subjected to the same loads as compared to reinforced concrete beams without shear connectors. The ferrocement formwork with and without shear connectors contributed about 21% - 75% and 16% - 50% to the flexural strength respectively.

In 1998 Afsaruddin and Hoque performed an experimental research work on reinforced concrete beams with ferrocement overlay in the concrete laboratory, BUET. They investigated the possibility of using ferrocement as a permanent formwork for reinforced concrete beams. A total of twelve beams were constructed

and tested in this investigation. Eight ferrocement beam formworks were made having different sizes. All of them were filled with reinforced concrete. Four reinforced concrete beams and eight reinforced concrete beams coated with ferrocement formwork containing single layer wire mesh were cast to compare the behavior of ferrocement formwork reinforced concrete beam with the normal reinforced concrete beam. The study demonstrates that the use of ferrocement a permanent formwork increases the cracking load and ultimate load of the composite system compared to normal RC beams. The number of cracks and width of cracks have been found to have reduced considerably due to the provision of ferrocement layer used as the formwork. From the study it appears that permanent precast ferrocement formwork could become a reliable alternative to wooden formwork in the construction of reinforced concrete beams.

2.5 Conclusion

Most of the above research works regarding the composite action of R.C. with ferrocement were limited to the evaluation of the performance or the structural effectiveness of R.C. with ferrocement. But the composite behaviour of ferrocement with Reinforced Concrete was not fully investigated and there is no definite guideline available for the analysis and design of a ferrocement coated R.C. beam. In this regard this study aims to propose a simple and direct analytical model to investigate the load-displacement behavior of such beams. The properties of ferrocement and the stress-strain behavior of concrete discussed in this chapter is used in formulating the analytical method.

Chapter 3

ANALYTICAL MODEL FOR FERROCEMENT-REINFORCED CONCRETE COMPOSITE BEAMS

3.1 Introduction

The flexure behavior of reinforced concrete beams with ferrocement overlay is investigated in this chapter. A simple and direct analytical procedure for evaluating the cracking and ultimate flexural capacities and corresponding deflections of a ferrocement RC composite beam is presented. The procedure is derived applying the basic principle of beam bending i.e., plane sections before bending remains plane and normal to the neutral surface after bending. Compatibility of strains are ensured between concrete and steel as in reinforced concrete and equations of equilibrium at a section are invoked to derive the stress and deflection equations. The results from this analytical procedure are compared with some previous experimental results and with the results obtained from linear finite element analysis of a ferrocement RC composite beam using the package, ANSYS.

3.2 Flexural Behavior of Ferrocement RC Composite Beams

The bending behavior of the ferrocement-reinforced concrete composite beam is quite different from the individual behavior of both reinforced concrete and the surrounding ferrocement layer. From several experimental investigations [Rosenthal and Bljuger,1985; Kaushik and Dubey,1994; Mays and Barnes,1995; Kadir,et.al.,1997] it has been found that a complete composite action between the ferrocement skin and the inner concrete core exists at least up to the first appearance of crack. Beyond that stage and up to failure, a partial separation may occur according to somewhat different crack patterns of the concrete core and the ferrocement overlay. But if full

bonding can be ensured at the RC and ferrocement interface through the use of mechanical connectors projected from the ferrocement forms or at least providing roughness to the contact surfaces of the ferrocement layer, then full composite action [Rosenthal and Bljuger,1985] can be obtained up to failure.

In the analytical study of the flexural behavior of the RC ferrocement composite beam, the cracking strength of the composite section is therefore determined from the flexural tensile strength of the ferrocement cover and the failure of the composite section under flexure will be governed by the strength of the reinforced concrete core. Theoretically, concrete resting on the ferrocement layer may crack before the cracking of the ferrocement layer. But here it will be assumed that the crack formation in the inner layer will not significantly affect the effectiveness of the concrete in the tension zone until the outer layer is cracked. The crack in the inner layer will not propagate significantly until the bottom ferrocement layer is cracked. From this consideration the first cracking moment of the composite section under flexure will be determined from the occurrence of the first crack in the ferrocement layer. Before the formation of the first flexural crack the behavior of all the materials is assumed to be linear and there exists a composite action between the core and the skin. Therefore, it is reasonable to assume a linear load displacement behavior of the composite beam before the formation of crack in the bottom ferrocement layer.

After the crack formation in the outer skin the mortar in the ferrocement can be assumed to be ineffective and the concrete in the tension zone will become ineffective gradually with further increase in the load. Therefore, in the postcracking service load stage the tensile strength of the composite section will depend on the tensile reinforcement in concrete and the wire mesh in the ferrocement layer. In the load-deflection response described in section 3.3.4, stage II reflects this condition. The stress-strain behavior of concrete in compression is still assumed to be linear. As the load continues to increase, the strain ε_s in the steel bars at the tension side continues to increase to reach the yield strain ε_y beyond which strain in steel is assumed to increase without any further increase in stress. In other words, reinforcing steel is assumed to be elastic and then perfectly plastic material. The beam is considered at this stage to have structurally failed by initial yielding of the tension steel. It continues to deflect

without additional loading, the cracks continue to open, and the neutral axis continues to rise toward the outer compression fibers. Finally a secondary compression failure develops, leading to total crushing of the concrete in the maximum moment region followed by rupture [Nawy, 1990].

3.3 Analysis of the RC Ferrocement Beam Section

An elastic-plastic section analysis for predicting the response of a rectangular, under-reinforced concrete beam with ferrocement overlay at the sides and bottom face, loaded statically in third-point bending to failure is performed. The analysis is based on the linear strain distribution in the cross section until failure and an idealized multilinear load-displacement curve shown schematically in Fig.3.4 is assumed. The actual load-displacement behavior of the beam is nonlinear. For simplicity the nonlinear curve is divided into three linear segments. The transition from one linear range to the other is assumed to depend on cracking of the ferrocement cover, change in stress-strain relationship of concrete and/or the reinforcing steel and the post yield failure behavior of the composite section.

3.3.1 Idealized Stress-strain Relationship of Concrete and Steel

In the sectional analysis of the RC ferrocement beam the stress-strain relationship of the individual materials concrete and steel are idealized as shown in Fig.3.1 and Fig.3.2 respectively. The nonlinear portion of the stress-strain curve is divided into linear segments in such a way that it is close to the actual non-linear response of the material.

The stress-strain curve for concrete is idealized as a trilinear curve (Fig.3.1). The first portion of the curve, to about 40% of the ultimate strength f'_c, can essentially be considered linear for all practical purposes. Beyond this point the curve becomes significantly nonlinear. And this nonlinear zone is divided into two linear segments — one upto the strain ε_{cy}, which is the strain in the concrete corresponding to the steel reaching its yield point and the other one is from ε_{cy} to the ultimate strain of concrete,

ε_c'. The strain ε_{cy} is dependent on the steel yield strain and the position of the neutral axis.

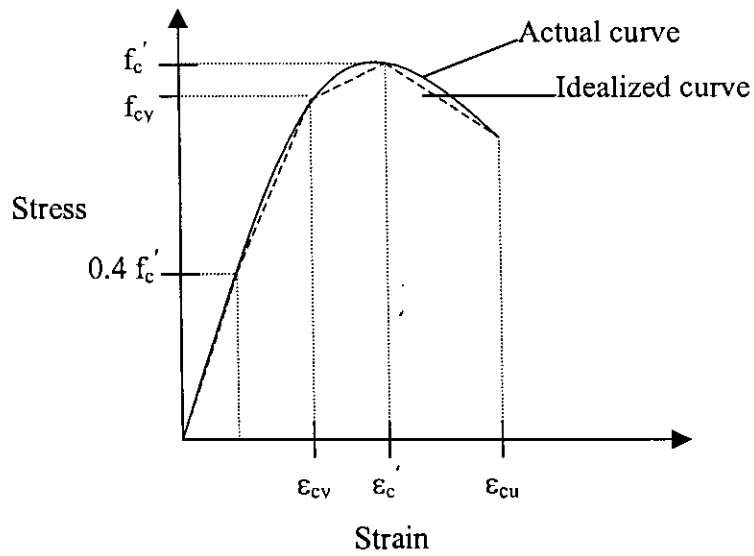

Fig.3.1 Typical and Idealized Concrete Stress-Strain Curve

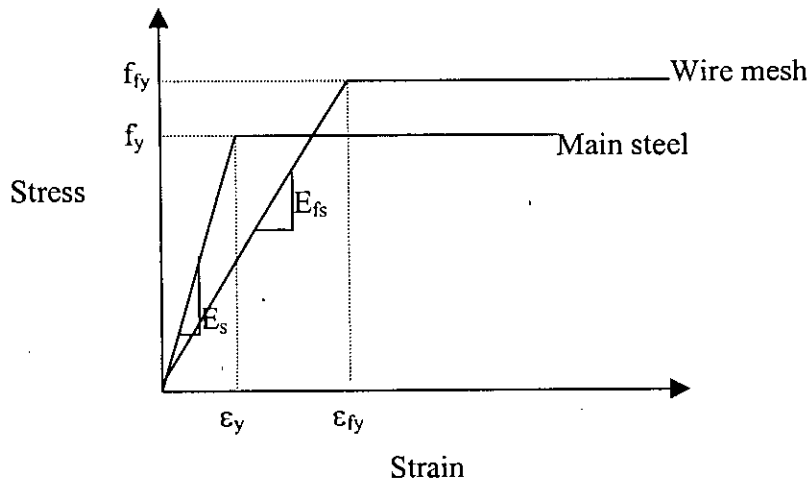

Fig. 3.2 Idealized Stress-Strain Curve for Tensile Steel

The overall stress-strain diagrams of steel and mesh reinforcement are idealized as a bilinear curve. The curve is assumed to be linear up to the yield point and after that the nonlinear portion is idealized as an average straight line (Fig.3.2) parallel to the x-axis. In the sectional analysis, the linear portion up to yield point of reinforcing steel

is used and the failure of the beam is assumed to initiate with the yielding of the main reinforcement.

3.3.2 Idealization of Ferrocement RC Composite Beam Sections

For the flexural analysis of the Ferrocement RC composite beam sections, the contribution of the vertical ferrocement layer is neglected and the effect of the vertical steels (stirrups) are also neglected. The effect of the vertical ferrocement layer will be considered in an approximate way by increasing the flexural tensile strength or modulus of rupture value due to the confinement effect of the inner concrete core surrounded by the outer ferrocement skin/layer. In all other analytical derivations of stresses, forces and moments there is no scope to incorporate the vertical layers' contribution explicitly. But in finite element analysis, the complete section of the beam is modeled in totality and both the contribution of vertical ferrocement layer and stirrups are incorporated in the analysis.

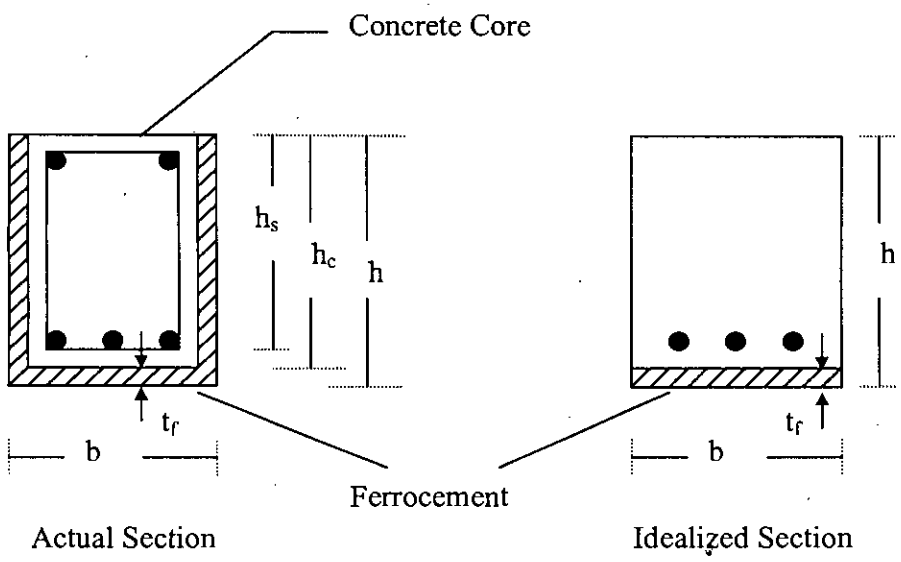

Fig.3.3 Idealization of the Ferrocement RC Composite Beam Section

3.3.3 Assumptions for the Analysis

The following assumptions are made in defining the behaviour of the composite section:

(a) Strain distribution is assumed to be linear. This assumption is based on Navier's hypothesis that plane sections remain plane and perpendicular to the neutral axis after bending.

(b) Strain in the steel and the surrounding concrete is the same prior to cracking of the concrete and at yielding of steel. That is perfect bond between steel and concrete is assumed.

(c) Perfect bond is assumed to exist at the interface of concrete and ferrocement as well.

(d) Ferrocement is assumed to act as a homogeneous elastic material before the occurrence of the first crack.

(e) Concrete and mortar is weak in tension. After cracking of the ferrocement layer, the mortar and the concrete in the tension zone becomes ineffective with further increase of load. Consequently in determining the ultimate moment capacity of the section and design computations, the mortar in the ferrocement layer and concrete in the tension zone of the section is neglected and the ferrocement wire mesh and the tension reinforcement is assumed to take the total tensile force.

3.3.4 Analysis of Sections

The analysis is based on linear strain distribution in the cross section until failure and a multilinear load-displacement curve of Fig.3.4. The load-displacement curve is divided into three linear regions as follows:

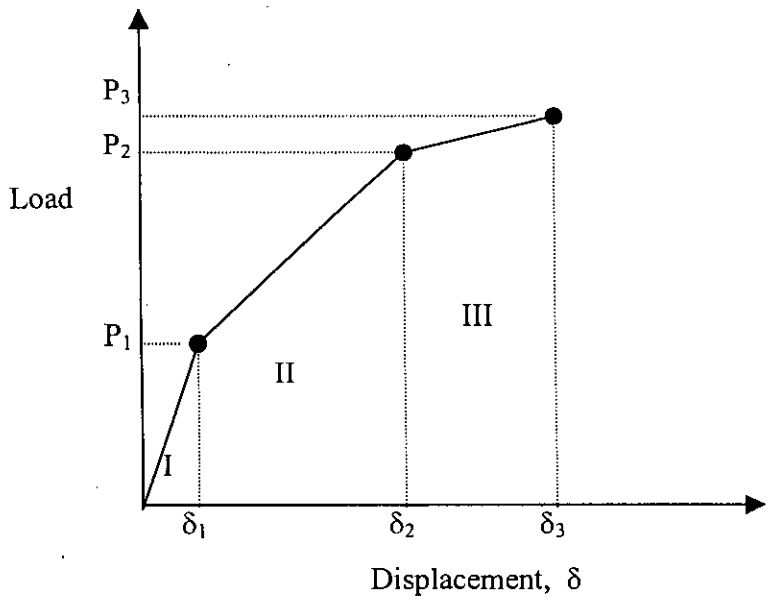

Fig.3.4: Idealized Load-Displacement Response for the Composite Section

(a) **Region I :** Precracking Stage
(b) **Region II :** Postcracking Serviceability Stage
(c) **Region III:** Postserviceability Cracking Stage or Ultimate Limit Stage

3.3.4.1 Precracking Stage: Region I

This region of the load-deflection curve is essentially a straight line defining full elastic behavior. The maximum tensile stress in the beam in this region is less than its tensile strength in flexure, namely, less than the modulus of rupture of ferrocement. The main features of this stage are:

(a) All material behavior is assumed to be elastic until tensile stress in the outer ferrocement layer reaches its modulus of rupture value.

(b) Before the formation of the crack the ferrocement layer will be assumed to act as a homogenous elastic material and its modulus of elasticity will be derived from Eq.(2.5).

(c) The flexural stiffness EI of the section can be estimated using Young's Modulus of elasticity E_c of concrete and the moment of inertia of the uncracked composite section.

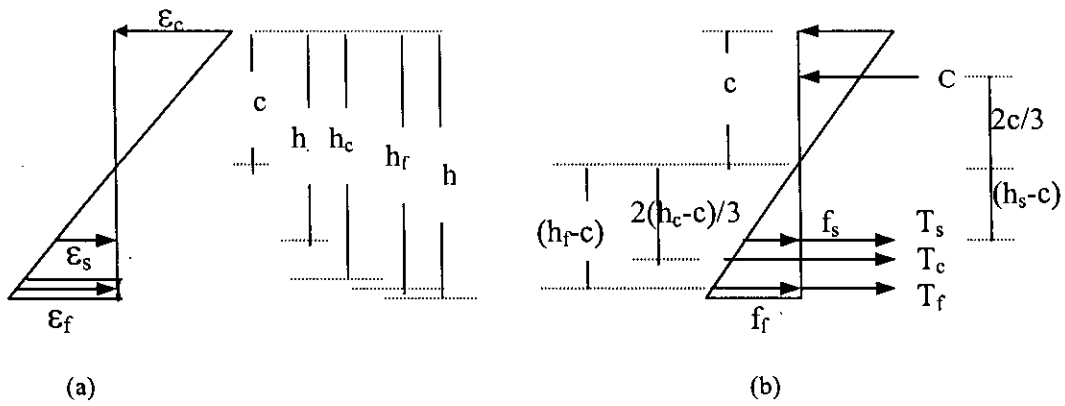

Fig.3.4 Strain and stress distribution diagram in the composite section for region I: (a) strain distribution and (b) stress and internal force distribution.

Referring to Fig.3.4(a), all the strains along the depth of the beam may be expressed in terms of the concrete strain at the compression face of the cross-section ε_c . Thus, the concrete tensile strain (ε_t) at the bottom of the concrete core, tensile strain in the main reinforcement (ε_s) and the strain in the ferrocement layer (ε_f) can be expressed as,

$$\begin{aligned} \varepsilon_t &= \varepsilon_c (h_c - c)/c \\ \varepsilon_s &= \varepsilon_c (h_s - c)/c \\ \varepsilon_f &= \varepsilon_c (h_f - c)/c \end{aligned} \tag{3.1}$$

where, c = distance of the neutral axis from the top of the section

h_c = depth of the concrete core

h_s = effective depth of the main reinforcement

h_f = effective depth of the ferrocement layer

Since, all material behavior in this region is assumed to be linear, the corresponding stresses can be expressed as the product of the strain and the respective modulus of elasticity. Thus, the forces acting on the cross-section (Fig.3.4(b)), can be expressed as,

Compression in concrete,

$$C = \varepsilon_c E_c (bc)/2 = \frac{1}{2} f_c bc \tag{3.2}$$

Tension in concrete,

$$\begin{aligned} T_c &= \frac{1}{2} b(h_c - c) f_{ct} \\ &= \frac{1}{2} b(h_c - c) \varepsilon_{ct} E_c \\ &= \frac{1}{2} b(h_c - c) \frac{\varepsilon_c (h_c - c)}{c} E_c \\ &= \frac{1}{2} b \frac{(h_c - c)^2}{c} f_c \end{aligned} \tag{3.3}$$

Tension in main reinforcement,

$$\begin{aligned} T_s &= A_s f_s \\ &= A_s (\varepsilon_s E_s) \\ &= A_s \frac{\varepsilon_c (h_s - c)}{c} E_s \\ &= A_s \frac{(h_s - c)}{c} \varepsilon_c (m_1 E_c) \\ &= m_1 A_s \frac{(h_s - c)}{c} f_c \end{aligned} \tag{3.4}$$

Tension in ferrocement cover,

$$
\begin{aligned}
T_f &= A_f\left(\varepsilon_f E_f\right) \\
&= A_f \frac{\varepsilon_c\left(h_f - c\right)}{c} E_f \\
&= A_f \frac{\varepsilon_c\left(h_f - c\right)}{c} m_2 E_c \\
&= m_2 A_f \frac{\left(h_f - c\right)}{c} f_c
\end{aligned}
\tag{3.5}
$$

where, $m_1 = E_s/E_c$ and $m_2 = E_f/E_c$

Assuming a condition of flexure without any axial force, the sum of the normal forces acting on the cross section must be zero, thus

$$\sum F = C - T_c - T_s - T_f = 0 \tag{3.6}$$

Substituting Eq.(3.2) through Eq.(3.5) into Eq.(3.6) and dividing by f_c yields,

$$
\begin{aligned}
&\Rightarrow \frac{1}{2}bc - \frac{1}{2}b\left(h_c - c\right)^2 - m_1 A_s \frac{h_s - c}{c} - m_2 A_f \frac{h_f - c}{c} = 0 \\
&\Rightarrow \frac{1}{2}bc^2 - \frac{1}{2}bc\left(h_c - c\right)^2 - m_1 A_s\left(h_s - c\right) - m_2 A_f\left(h_f - c\right) = 0
\end{aligned}
$$

After simplification the expression for the position of neutral axis c becomes,

$$c = \frac{\frac{1}{2}bh_c^2 + h_s m_1 A_s + h_f m_2 A_f}{bh_c + m_1 A_s + m_2 A_f} \tag{3.7}$$

The slope of the load-displacement curve i.e. stiffness of the composite beam in this region may be written as,

$$k_1 = (P/\delta)_1 = K(EI)_1 \tag{3.8}$$

where, $(EI)_1$ is the flexural rigidity of the uncracked cross section in Region I and $K=1296/23L^3$ is a constant obtained in the derivation of the beam midspan deflection for third point bending used in the beam tests. The flexural rigidity $(EI)_1$ of the composite section can be expressed in terms of the neutral axis distance c as,

$$(EI)_1 = E_c\frac{bc^3}{3} + E_c b\frac{(h_c - c)^3}{3} + E_s A_s (h_s - c)^2 + E_f A_f (h_f - c)^2 \tag{3.9}$$

and the moment of inertia of the composite section is determined from the relation,

$$I_1 = \frac{(EI)_1}{E_c} \tag{3.10}$$

For third point bending the maximum bending moment M_1 and corresponding load P_1 are related as,

$$M_1 = \frac{P_1 L}{6} \tag{3.11}$$

where, P_1 is the total load on the beam i.e., the sum of the two third point loads. The first cracking moment i.e. the moment at the end point of region I can be determined from the elastic flexure formula using the modulus of rupture value of the outer ferrocement layer,

$$f_{rf} = \frac{M_1(h-c)}{I_1} = \frac{P_1 L(h-c)}{6I_1} \tag{3.12}$$

Having established the first cracking load P_l from Eq.(3.12), the corresponding beam deflection δ_1 is determined from,

$$\delta_1 = \frac{P_1}{k_1} \tag{3.13}$$

Here, P_l and δ_l indicates the coordinates of the end point (P-1) of region I on the schematic load-deflection curve presented in Fig.3.4.

3.3.4.2 Postcracking Service Load Stage: Region II

The precracking region ends at the initiation of the first crack in the ferrocement layer and moves into region II of the load-deflection diagram in Fig.3.4 with further loading. Most beams lie in this region at service loads. A beam undergoes varying degrees of cracking along the span corresponding to the stress and

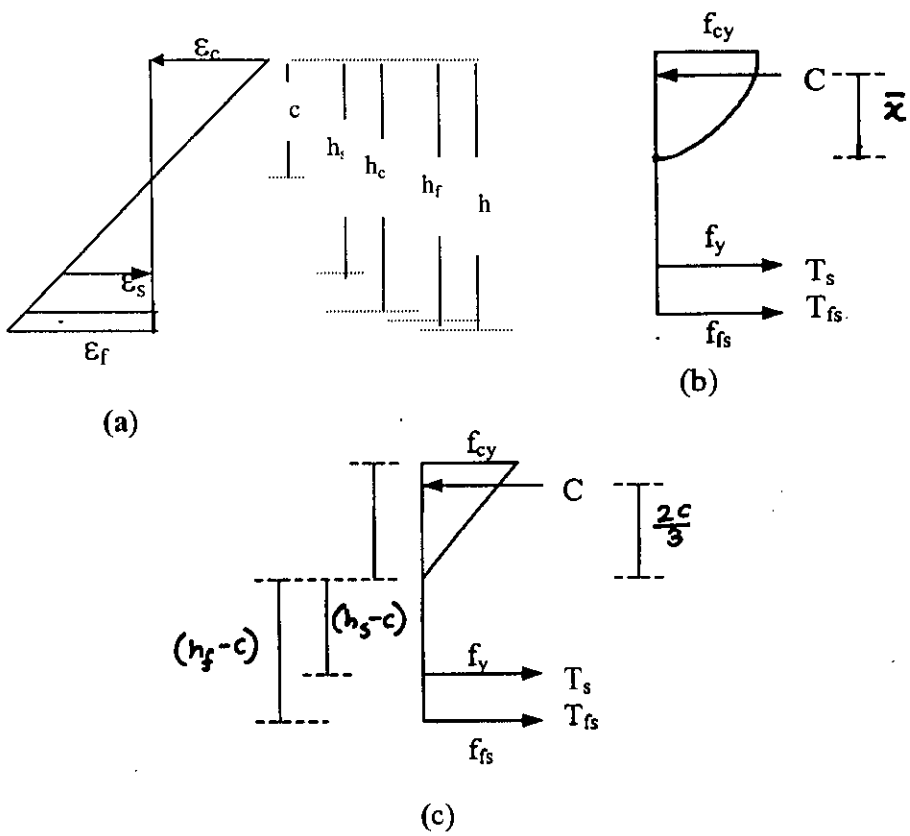

Fig.3.6 Assumed strain and stress distribution in the composite section for region II: (a) strain distribution, and (b) nonlinear stress distribution, and (c) linear stress distribution.

deflection levels at each section. Hence flexural cracks are wider and deeper at midspan, whereas only narrow minor cracks develop near the supports in a simple beam. But cracks due to diagonal tension is severe near the supports and in that case the contribution of vertical ferrocement layer is quite significant in delaying the formation of such cracks.

The main features of this region:

(a) The mortar in the ferrocement becomes ineffective due to the crack formation in the ferrocement layer and the effective area of reinforcement in the cracked ferrocement layer is determined using Eq.(2.4).

(b) The concrete below the neutral axis also becomes ineffective gradually with the increasing load (or increasing number and width of cracks).

(c) Distribution of compressive stress in the concrete above the neutral axis becomes nonlinear as in Fig.3.6(b). The resultant compressive force in concrete is calculated using Eq.(2.8) as described in chapter two.

(d) This loading region ends with the yielding of the main tension reinforcement of the beam.

To determine the bending moment M_2 and load P_2 the strains at different levels in the section is expressed in terms of the yield strain of the main reinforcement. Referring to Fig.3.6(a) the strains at different levels are,

$$\begin{aligned} \varepsilon_c &= \varepsilon_y c/(h_s - c) \\ \varepsilon_s &= \varepsilon_y \\ \varepsilon_f &= \varepsilon_y (h_f - c)/(h_s - c) \end{aligned} \tag{3.14}$$

The equilibrium forces acting in the section is evaluated to determine the location of the neutral axis. The resultant compression in the concrete for a rectangular section can be calculated using Eq.(2.8) as described in chapter 2.

$$C = bf_c^{'} \frac{\phi}{\varepsilon_c^{'}} c^2 \left[1 - \frac{\phi c}{3\varepsilon_c^{'}} \right]$$

$$= bf_c^{'} \frac{\varepsilon_y}{\varepsilon_c^{'}(h_s - c)} c^2 \left[1 - \frac{\varepsilon_y c}{3\varepsilon_c^{'}(h_s - c)} \right] \tag{3.15}$$

where, ϕ = slope of the strain-distance diagram (Fig.3.6(a))

The tension forces acting on the section,

$$T_c = 0$$

$$T_s = A_s f_y \tag{3.16}$$

$$T_f = A_{fs}(\varepsilon_f E_f)$$

$$= A_{fs} \frac{\varepsilon_y (h_f - c)}{(h_s - c)} E_{fs}$$

$$= A_{fs} \frac{\varepsilon_y (h_f - c)}{(h_s - c)} m_3 E_c$$

$$= m_3 A_{fs} \frac{(h_f - c)}{(h_s - c)} \varepsilon_y E_c \tag{3.17}$$

where, $m_3 = E_{fs}/E_c$

Applying equilibrium equation to find the location of the neutral axis c,

$$C = T_C + T_s + T_f$$

$$\Rightarrow bf_c^{'} \frac{\varepsilon_y}{\varepsilon_c^{'}(h_s - c)} c^2 \left[1 - \frac{\varepsilon_y c}{3\varepsilon_c^{'}(h_s - c)} \right] = A_s f_y + m_3 A_{fs} \frac{(h_f - c)}{(h_s - c)} \varepsilon_y E_c \tag{3.18}$$

This higher order equation of c is solved by trial and error method. In first trial the value of c is assumed to be $0.6c_1$, where c_1 is the neutral axis position found in stage I of the load-displacement diagram.

To make the determination of c more simple another analysis was done assuming linear variation of the stress-distribution diagram in compression as shown in Fig 3.5(c). In this case the modulus of elasticity is considered to be equal to the secant modulus value as used in stage I. The value of c found from the linear stress distribution (Fig.3.4(c)) was found to be around 98% of the value found from nonlinear stress-distance diagram. Therefore, it is proposed that a linear stress-distance diagram for concrete in compression zone upto the strain ε_{cy} may be used without loss of significant accuracy.

For linear stress variation the total compressive stress acting in the section will become,

$$\begin{aligned} C &= \varepsilon_c E_c (bc)/2 \\ &= \frac{1}{2} bc^2 \frac{\varepsilon_y}{(h_s - c)} E_c \\ &= \frac{1}{2m_1(h_s - c)} bc^2 f_y \end{aligned} \tag{3.19}$$

Thus the equilibrium equation in this case results in a quadratic equation in c expressed as,

$$\begin{aligned} &\Rightarrow \frac{1}{2} bc^2 \frac{\varepsilon_y E_c}{(h_s - c)} - m_1 A_s \varepsilon_y E_c - m_3 A_{fs} \frac{h_f - c}{(h_s - c)} \varepsilon_y E_c = 0 \\ &\Rightarrow \frac{1}{2} bc^2 - m_1 A_s (h_s - c) - m_3 A_{fs} (h_f - c) = 0 \\ &\Rightarrow c^2 + \frac{2}{b}(m_1 A_s + m_3 A_{fs})c - (m_1 A_s h_s + m_3 A_{fs} h_f) = 0 \end{aligned} \tag{3.20}$$

c can be determined explicitly solving this quadratic equation Eq.(3.20) and the moment about the neutral axis M_2 may be determined as,

$$M_2 = C\bar{x} + T_s(h_s - c) + T_f(h_f - c) \tag{3.21}$$

where,

$$\bar{x} = c\left[\frac{8\varepsilon_c' + 3\phi c}{12\varepsilon_c' - 4\phi c}\right] \quad \text{for nonlinear stress distribution}$$

$$\bar{x} = \frac{2c}{3} \quad \text{for linear stress distribution}$$

and the load P_2 is determined from,

$$P_2 = 6M_2/L \tag{3.22}$$

Flexural rigidity of the section is determined neglecting the concrete below the neutral axis as,

$$(EI)_2 = E_c bc^3/3 + E_s A_s(h_s - c)^2 + E_{fs} A_{fs}(h_f - c)^2 \tag{3.23}$$

Therefore, the slope of the load-displacement curve becomes,

$$k_2 = (P/\delta)_2 = K(EI)_2 \tag{3.24}$$

The increase in displacement from point 1 to point 2 is determined from,

$$\Delta_2 = (P_2 - P_1)/k_2 \tag{3.25}$$

The total deflection δ_2 at the end of this region is obtained as,

$$\delta_2 = \delta_1 + \Delta_2 \tag{3.26}$$

3.3.4.2 Post Serviceability or Ultimate Limit Stage : Region III

The load-deflection curve (Fig.3.4) becomes considerably flatter in region III than in the preceding regions. This is due to substantial loss in stiffness of the section because of extensive cracking and considerable widening of the stabilized cracks throughout the span. At this stage the beam is considered to have failed considering serviceability limit state due to initial yielding of the main tension reinforcement. It continues to deflect without significant additional loading, the cracks continue to open, and the neutral axis continues to rise toward the outer compression fibers. Finally, a secondary compression failure develops, leading to total crushing of the concrete in the maximum moment region followed by rupture.

In this region the steel behavior is inelastic, having reached its work hardening portion of the stress-strain curve shown in Fig.3.2. At the end of this region (Point 3) the concrete compressive stress reaches its ultimate value f_c' and the associated strain ε_c' is also attained. However failure is assumed to be delayed until concrete extreme fiber strain reaches the crushing strain, ε_{cu}. To determine the neutral axis position, the nonlinear concrete compressive stress distribution is replaced by an equivalent rectangular stress block as proposed by Whitney and

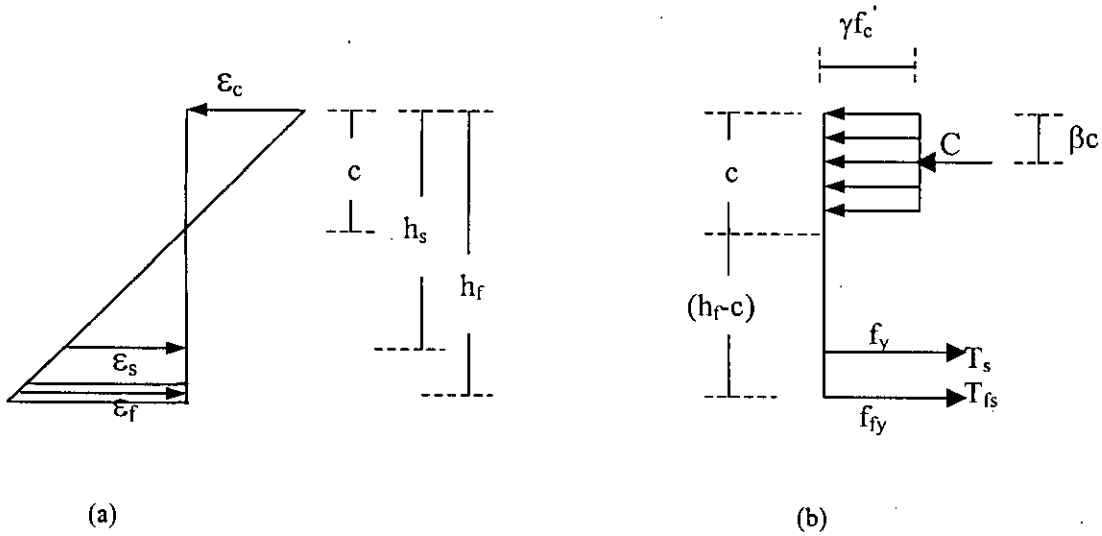

Fig.3.7 Assumed strain and stress distribution in the composite section for region III: (a) strain distribution, and (b) stress and internal force distribution.

adopted by different code of practices like ACI 318-83. The position of the concrete compressive force is shown in Fig.3.7(b) and its magnitude is given as,

$$C = \gamma f_c' 2 \beta bc \tag{3.27}$$

where γ and β are two empirical constants (Nilson,1997) used in defining the equivalent rectangular stress block.

Tension in the main reinforcement and in the ferrocement mesh are expressed as,

$$\begin{aligned} T_s &= f_s A_s \\ T_f &= f_{fs} A_{fs} \end{aligned} \tag{3.28}$$

Using the linear stress-strain distribution shown in Fig.3.7 the strains in the main reinforcement and in the ferrocement mesh become,

$$\begin{aligned} \varepsilon_s &= \varepsilon_{cu}(h_s - c)/c \\ \varepsilon_{fs} &= \varepsilon_{cu}(h_f - c)/c \end{aligned} \tag{3.29}$$

In the idealized stress-strain diagram for steel and wire mesh it is assumed that in the inelastic range i.e. after yielding there will be no increase in the stress of the material with the increasing value of strain. The stress-strain diagram becomes a straight line parallel to the x-axis. Now the main reinforcement is assumed to yield at the end of region II but as the modulus of elasticity of square wire mesh is much lower [ACI Committee Report 549, 1993] than main reinforcement, it will yield later. In region III, if the value of the strain in the wire mesh exceeds the yield strain value the stress in the wire mesh will be taken equal to its yield stress otherwise the stress will be determined from the linear relationship of stress and strain. Therefore the tension forces will become,

$$T_s = f_y A_s$$

$$T_f = \varepsilon_{fs} E_{fs} A_{fs} \qquad if, \varepsilon_{fs} < \varepsilon_{fy} \qquad (3.30)$$

$$or, T_f = f_{fy} A_{fs} \qquad if, \varepsilon_{fs} \geq \varepsilon_{fy}$$

Summing the forces C, T_s and T_f,

$if \varepsilon_{fs} < \varepsilon_{fy}$,

$$\alpha f_c' bc - f_y A_s - \frac{\varepsilon_{cu}}{c}(h_f - c) E_{fs} A_{fs} = 0$$

$$\Rightarrow \alpha f_c' bc^2 - (f_y A_s - \varepsilon_{cu} E_{fs} A_{fs}) c - \varepsilon_{cu} h_f E_{fs} A_{fs} = 0 \qquad (3.31)$$

$if \varepsilon_{fs} \geq \varepsilon_{fy}$,

$$\alpha f_c' bc - f_y A_s - f_{fy} A_{fs} = 0$$

$$\Rightarrow c = \frac{f_y A_s + f_{fy} A_{fs}}{\alpha f_c' b} \qquad (3.32)$$

Position of the neutral axis can be determined from Eq.(3.31) or Eq.(3.32) and the ultimate moment capacity of the section is calculated as,

$$M_3 = C(1 - \beta)c + T_s(h_s - c) + T_f(h_f - c) \qquad (3.33)$$

Ultimate load P_3 is therefore,

$$P_3 = 6M_3 / L \qquad (3.34)$$

The flexural rigidity of the cross-section is assumed to be developed by main tension steel and the wire mesh reinforcement only. Contribution of the concrete in the compression side is therefore neglected for simplicity. In reality, this bending stiffness only defines the slope of the load deflection curve beyond P_3, and is expressed as,

$$(EI)_3 = E_s b(h_s - c)^2 + .E_{fs} A_{fs} (h_f - c)^2 \tag{3.35}$$

The slope of the load-displacement curve in this region is,

$$k_3 = (P/\delta)_3 = K(EI)_3 \tag{3.36}$$

Increase in the displacement beyond Point 2 is,

$$\Delta_3 = P_3/k_3 \tag{3.37}$$

and the displacement at Point 3 becomes,

$$\delta_3 = \delta_2 + \Delta_3 \tag{3.38}$$

3.4 Analysis of a Typical RC Beam with Ferrocement Overlay

To illustrate the above procedure of determining the load-deflection response of a reinforced concrete beam with ferrocement overlay a typical simply supported RC (reinforced concrete) beam encased in U-shape ferrocement cover (Fig.3.8) is analysed using the proposed analytical model. Cross-sectional dimensions and reinforcement details of the beam are shown in Fig.3.8. In the 20 mm outer ferrocement cover single layer of square woven mesh with 11.4mm× 11.4 mm mesh opening and 1.2 mm wire dia is used. The idealized section for the analytical model is given in Fig.3.9. The beam is analyzed for two point loading i.e. under pure flexural condition.

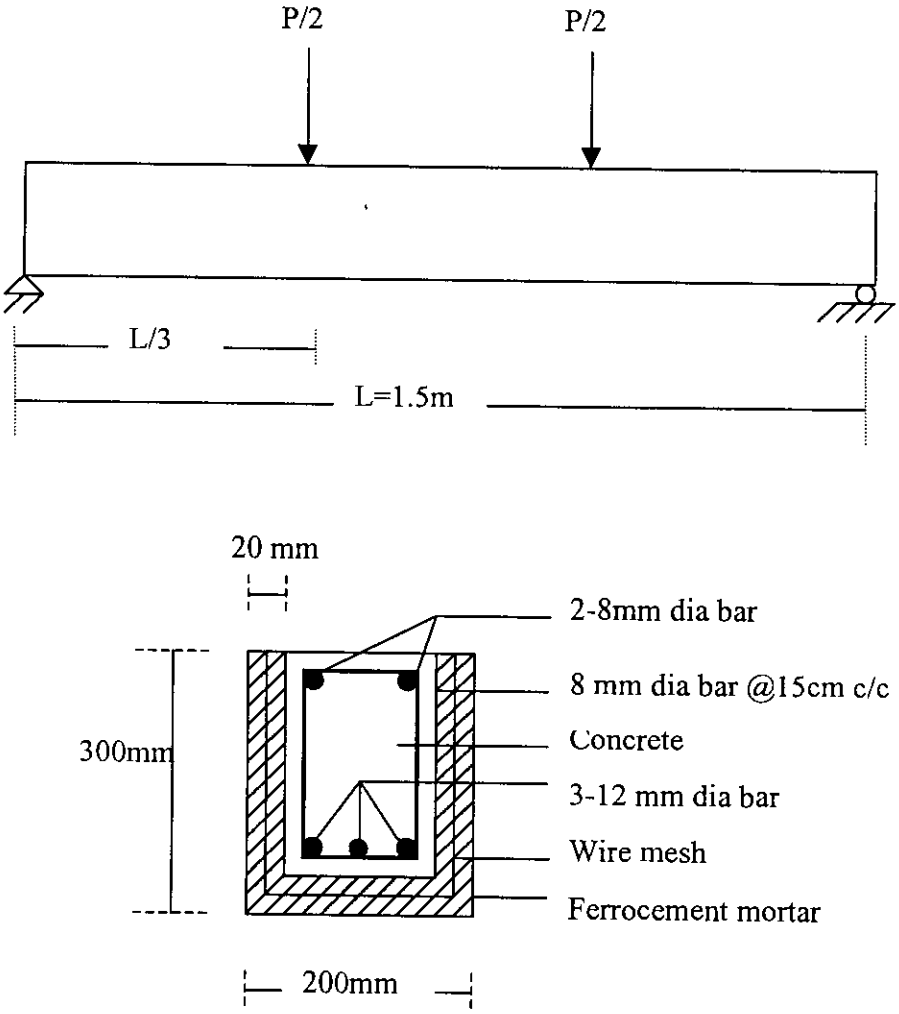

Fig.3.8 A Typical Reinforced Concrete Beam with Ferrocement Overlay

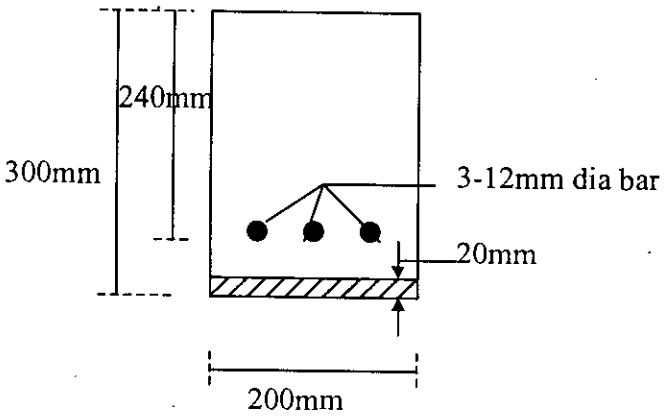

Fig. 3.9 Idealized Section for Analytical Analysis

Volume fraction of the square woven mesh used in the ferrocement cover is found to be 0.99% (Eq.2.1) and corresponding first cracking stress for the ferrocement cover is 5.27 Mpa (Eq.2.6). First cracking moment for the beam in flexure is determined from Eq.3.12 for the first cracking stress in the ferrocement layer. The load and deflection values at the end of each region of the idealized load-deflection curve is calculated using the derived expressions for the analytical model. Calculations and results are summarised in Table 3.1 and the idealized load-deflection curve is shown in Fig.3.10.

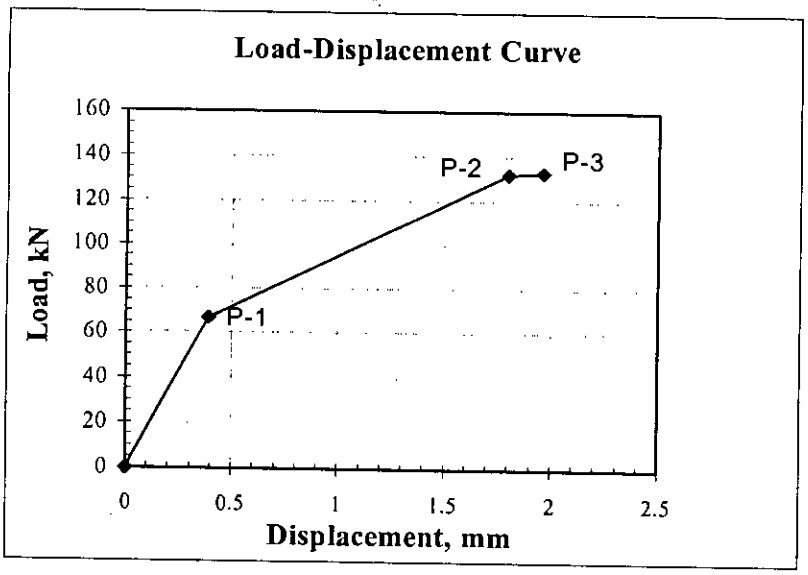

Fig.3.10 Load-Displacement Curve for the Typical Beam

Table 3.1 Summary of the Analysis of the Typical RC Ferrocement Beam

Parameters	Region I	Region II		Region III
		Linear stress distribution	Nonlinear stress distribution	
Location of the neutral axis, c (mm)	153	70.2	71.3	37.7
Flexural Rigidity, EI ($N\text{-}mm^2$)	1.15E+13	2.71E+12	2.71E+12	1.84E+12
Maximum Moment, M (kN-m)	16.64	32.94	33.16	34.32
Maximum Load, P (kN)	66.56	131.76	132.64	137.28
Stiffness or slope of the P-δ curve, k (kN/m)	192599	45281	45288	30766
Deflection, δ (mm)	0.346	1.79	1.80	1.96

3.5 Conclusion

The analytical method described in this chapter for predicting the load-displacement response of ferrocement coated reinforced concrete beam under flexure is simple and direct and can be used to predict the serviceability and the ultimate behavior of the composite beam. Verification of the proposed analytical method is done by comparing the analytical results of the section analysis with some existing experimental results and also with the results obtained from finite element analysis of the composite section using the package, ANSYS. The method is then used to analyze three sets of beams to observe the effect of number of mesh layers and thickness of the ferrocement cover on the behavior of the composite beam.

Chapter 4

FINITE ELEMENT ANALYSIS

4.1 Introduction

With the advent of sophisticated numerical tools for analysis like the finite element method (FEM), it has become possible to model the complex behavior of reinforced concrete beams encased in ferrocement. In this study a linear finite element analysis using the package ANSYS, was performed to predict the elastic behavior of the composite beam upto cracking and to observe the confinement effect of ferrocement cover on the reinforced concrete core. Detailed description of finite element modeling of the composite beam section and the steps followed in the analysis using ANSYS are given in the following article. The entire material behavior is assumed to be linearly elastic in finite element analysis performed in this study.

4.2 An Overview to ANSYS

The ANSYS computer program is a large-scale general-purpose finite element program that is used for solving several classes of engineering analysis. Its capabilities range from simple linear static analysis to a complex nonlinear, transient, dynamic analysis. The ANSYS element library contains more than fifty elements for static and dynamic analysis, over twenty for heat transfer analysis, and includes several magnetic, field, and special purpose elements. This variety of elements allows the ANSYS program to analyze two and three dimensional frame structures, piping system, 2-dimentional plan and axisymmetric solids, 3-dimensional solids, flat plates, axisymmetric and 3-dimentional shell and nonlinear problems including gaps (interface) and cables.

The input data for an ANSYS analysis are prepared using preprocessors. The general preprocessors (PREP7) contains powerful solids modeling and mesh generation capabilities, and is also used to define all other analysis data (geometric properties,

real constants, material properties, constraints, loads, etc.) with the benefit of database definition and manipulation of analysis data. Extensive graphics capabilities is available through out the ANSYS program, including isometric, perspective, section, edge, and hidden-line displays of 3-dimentional structure, X-Y graph of input quantities and results, and other contour displays of solution of results. A load-history pre-processor (PREP6) is available for creating transient or sequential loading and boundary condition.

A typical ANSYS analysis has three distinct steps:

- Build the model.
- Apply loads and obtain the solution.
- Review the results.

Building a finite element model requires more of an ANSYS user's time than any other parts of the analysis.At first a job name and a "title of the analysis" needs to be specified. Then the element types, element real constants, material properties and model geometry are defined. Most element types require material properties. Depending on the application, material properties may be a) linear or non-linear b) isotropic, orthotropic, anisotropic and c) constant temperature or temperature depended. Once material properties have been defined, the next step in an analysis is generating a FE model with nodes and elements that adequately describe the model geometry. After obtaining the solution the result of the ANSYS analysis can be reviewed with postprocessors.

The ANSYS program has a comprehensive graphical user interface (GUI) that gives user easy, interactive access to program functions, commands, documentation, and reference material. An intuitive menu system helps user navigate through the ANSYS program. Users can input data using a mouse, a keyboard, or a combination of both.

4.3 Finite Element Modeling of Reinforced Concrete

Finite Element Modeling of a reinforced concrete element is not much easier as it is composed of two different types of materials—concrete and steel. In most of the models of reinforced concrete beams concrete and steel are usually defined as separate elements. Concrete is defined by 2-D plane elements or 3-D solid elements and steels are embedded in concrete with the help of link elements. At the interface of concrete and steel, spring elements are used to simulate the bond slip between the reinforcement and surrounded concrete. But this method of modeling using link elements is cumbersome and time consuming. To avoid this complicity and to simulate the behavior of both steel and concrete in one model, an attempt has been made in this study to develop a more generalized finite element modeling of reinforced concrete with layered composite solid element, from ANSYS element library. And the results of the analysis using this layered system is than compared with the theoretical ones to observe the validity of the finite element model.

4.3.1 Element Type Adopted

Solid 46 3-D layered structural solid element from ANSYS element library has been selected for the modeling of the composite Beam section. This is a 8-noded structural layered solid element (Fig.4.1) which can accommodate 100 different material layers. The element has three degrees of freedom at each node: translations in the nodal x, y, and z directions. A composite section can be easily modeled with the help of this element by simply defining the material properties and thickness for each layer. The essential features of this element are discussed below.

4.3.2 Input Data

The geometry, node locations, and the coordinate system for this element are shown in Fig.4.1. The element is defined by eight nodes, layer thickness, layer material direction angles and material properties. The element z-axis is defined normal to a flat reference plane, using real constant KREF as shown in Fig.4.1. The default

element x-axis is the projection of side I-J, side M-N, or their average (depending on KREF) on to the reference plane. The material properties of each layer may be orthotropic in plane of the element. The real constant MAT is used to define the layer material number instead of the element material number applied with the MAT command (ANSYS 5.4, Help System).

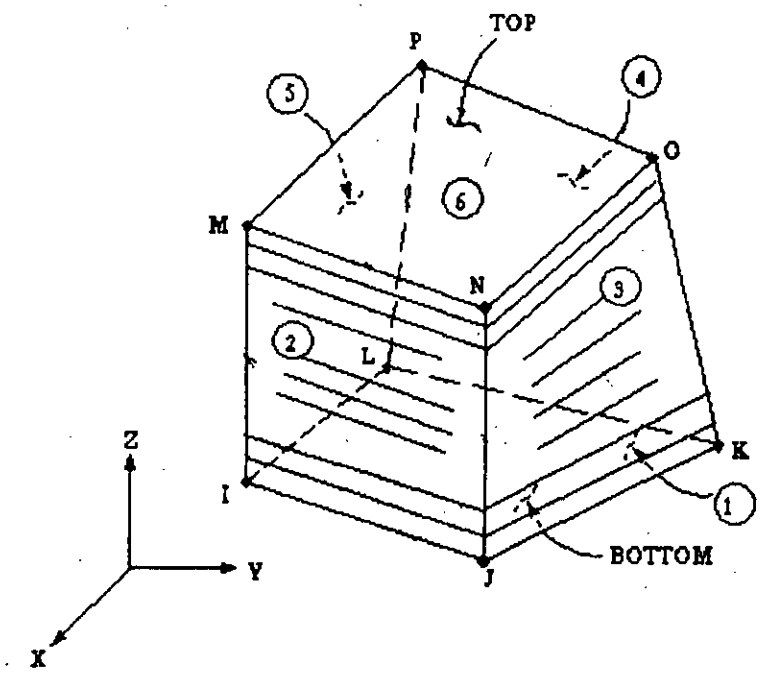

Fig.4.1: SOLID 46 3-D Layered Structural Solid

4.3.3 Output Data

The solution output associated with the element in two forms:

- Nodal solution
- Element solution

Both include stresses, forces, displacements etc. at the nodal points. The contour plot of the results can also be viewed using plot results.

4.3.4 Assumptions and Restrictions

Zero volume elements are not allowed. This occurs most often whenever the elements are not numbered properly. All elements must have eight nodes. Zero thickness layers or layers tapering down to zero thickness at the corner are not allowed. No slippage is assumed between the element layers. All material orientations are parallel to the reference plane. This element is limited to 20 constant thickness layers, or 10 tapered layers. The damp material property is not allowed.

4.3.5 Modeling of the Reinforcement

In a finite element model of a reinforced concrete member, reinforcements can be represented in one of the following three forms—distributed, embedded and discrete (Task Committee on Finite Element Analysis, 1982) . The first method is adopted in this study where the steel is assumed to be distributed over the concrete element, with a particular orientation angle. A composite concrete-reinforcement constitutive relation is used in this case. To derive such a relation, perfect bond must be assumed between the concrete and steel. In embedded representation the reinforceing bar is considered to be an axial member built into the isoparametric element such that its displacements are consistent with those of the element. Again perfect bond must be assumed. Whereas in discrete representation of reinforcement axial force members or bar links may be used and can account for possible displacement of the reinforcement with respect to the surrounding concrete. But in modeling of reinforcement using discrete system one has to maintain the track of the nodes where the reinforcements are connected very carefully. Several studies have been performed using this discrete system. In this study the distributed scheme was followed to model the main horizontal reinforcements and stirrups in the concrete core and the reinforcing mesh in the ferrocement cover to observe the performance of this simplified model of the composite beam under flexure.

4.3.5.1 Horizontal Reinforcement

Main longitudinal bottom bars and the top bars, of a reinforced concrete beam section is modeled as equivalent horizontal steel layers with concrete layers at the

top and bottom of the corresponding steel layer. The thickness of the layer is determined dividing the area of the reinforcement by the width of the element.

The wire mesh in the bottom ferrocement layer is also modeled as horizontal steel layer. And the equivalent thickness is determined from the mesh geometry and the diameter of the wires. For multiple layer wire mesh the layer thickness is equivalent to the thickness of the single layer wire mesh multiplied by the number of layers with in the ferrocement cover.

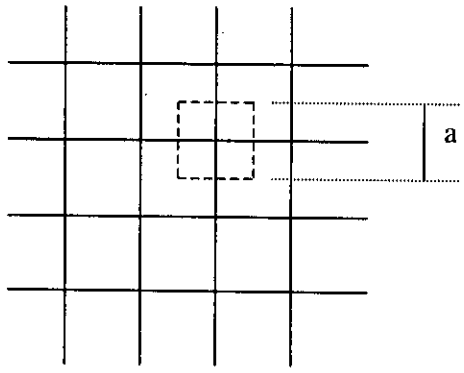

Fig.4.2: A Typical Square Mesh

For a square opening wire mesh the thickness of the steel layer can be determined as,

$$t_w = \frac{\pi d^2}{4a} \times N$$

where, d = diameter of the wire

a = center to centre distance of wires

N = no of mesh layers

The horizontal layers are defined in the global xy plane and thickness of the layers is defined along the z-axis. Isotropic material properties of steel were used in defining the material properties for each layer. A typical layerd model of a reinforced concrete beam is shown in Fig. 4.4.

4.3.5.2 Vertical Reinforcement

The wire mesh in the vertical ferrocement layer and the stirrups in the reinforced concrete core is represented with vertical steel layers. To change the layer direction from horizontal to vertical the element co-ordinate system was just oriented 90° and the element is defined choosing the nodes in such a way that the layers of the element will be parallel to the global vertical direction. To introduce these vertical reinforcements in the model the element co-ordinate system is just rotated through 90 degrees and the element is defined choosing the nodes in such a way that the layers of the element be parallel to the global vertical direction. Therefore, finite element modeling of the composite section is performed discretizing it into several horizontal and vertical layered elements.

The main objective of providing stirrups is to resist diagonal cracks due to shear stresses. It is assumed that the vertical stirrups resists only the vertical tensile stresses developed in the section due to shear. In the 3-D model of the composite beam the vertical steel layer properties should be so modeled that this behavior is truly reflected. To simulate this behavior the vertical steel layer is defined with orthotropic material properties i.e. modulus of elasticity will be different in the three different co-ordinate directions for the vertical layer. In ANSYS material properties are always defined in the local coordinate system of the element. In case of layered elements the material X direction corresponds to the local layer X direction. Again the local X direction for the vertical layers corresponds to the global vertical (Z) direction for the complete model. Therefore, to represent the behavior of shear reinforcements in the vertical steel layers the value of E_x will be defined as the actual value of the modulus of elasticity of steel and values of E_y and E_z will be assigned a negligible value other than zero. As zero values for these properties are not valid for orthotropic material properties defined in ANSYS.

4.3.6 Modeling of the Composite Beam

A reinforced concrete beam encased in U shape ferrocement cover is modeled using the (layered) finite element package ANSYS to observe flexural behavior of the

composite section up to cracking. At first, the beam is divided into finite number of segments (Fig.4.3) along the span of the beam. Then each segment is discretized into six Solid 46-3D layered element as shown in Fig. 4.4. Three elements were used to model the inner concrete core and three for the outer ferrocement cover. The number of element may be increased depending on the dimensions of the section and considering the shape factors of the elements. All the elements are connected at the nodes. Total 14 nodes are needed to discretize the section into six elements.

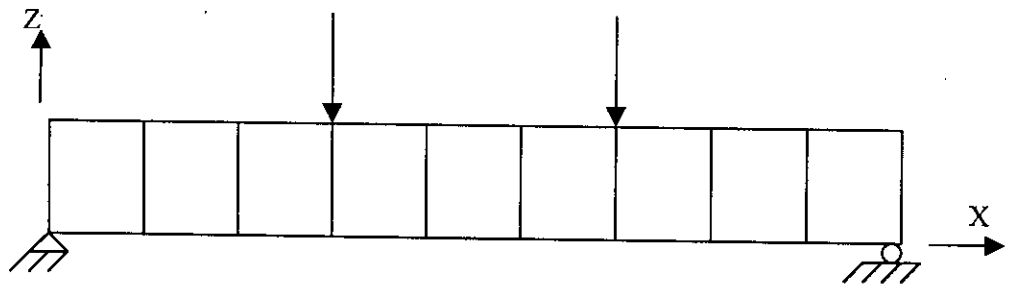

Fig.4.3: A Typical Beam Discretized into Finite Number of Segments for Analysis

The inner concrete core is descritized into one element with horizontal layer and two elements with vertical layers. Five horizontal layers of different thickness are provided in the horizontal layered element—three concrete layers and two steel layers. The vertical layered elements at the two sides are defined with two layers —one concrete and one steel layer for stirrups. The outer U-shape ferrocement cover is divided into one horizontal and two vertical elements. Each of these elements are defined with two mortar layer and a steel layer for the wire mesh at the center of the element (Fig.4.4). Global coordinate directions are also shown in the figures.

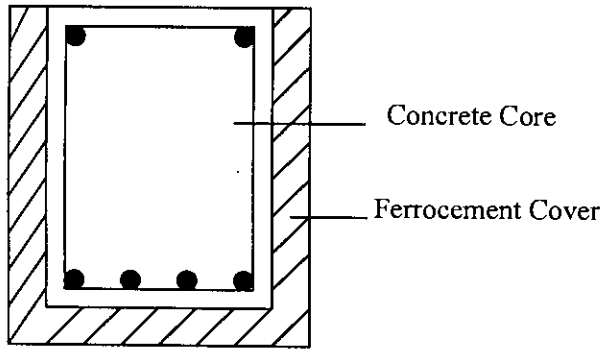

Fig.4.3: A Typical Reinforced Concrete Section with Ferrocement Overlay

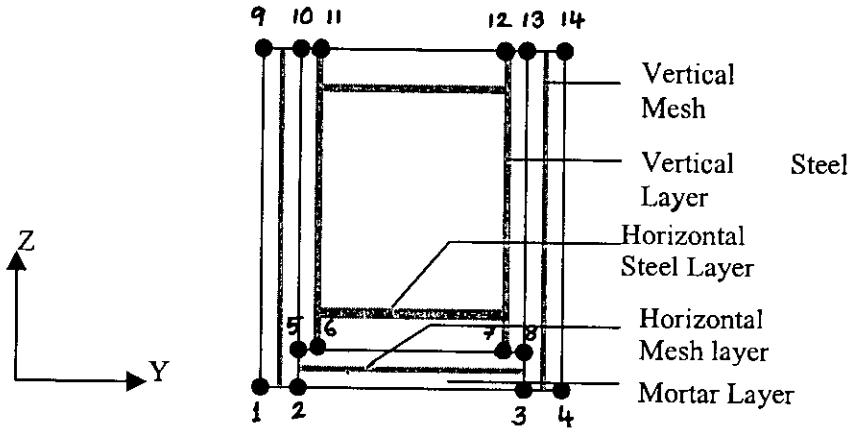

Fig.4.4: Finite Element Model of the Composite Section using Layered Element

4.5 Performance of the Finite Element Model

To investigate the performance of the finite element model using layered element, the typical RC (reinforced concrete) ferrocement composite beam is modeled and analyzed with ANSYS. The beam is analyzed for two point loading i.e. under pure flexural condition. The 3-D finite element model build in ANSYS is shown in Fig.4.5, 4.6 and 4.7. The material properties defined for each material layer is summarized in Table 4.1. Mainly three types of materials are used—concrete, mortar and steel. Again steel is defined with three different properties for different steel layers. Horizontal main reinforcements are defined with isotropic steel properties whereas the vertical steel layers are defined with orthotropic properties of steel to represent the behavior of stirrups as discussed before. Steel layer for wire mesh reinforcements are defined with the properties of mesh reinforcements according to the minimum values recommended in ACI manual.

Table 4.1: List of Material Properties used in the Finite Element Analysis

Material	Type	E_x (MPa)	E_y (MPa)	E_z (MPa)	ν
Concrete	Isotropic	25000	25000	25000	0.17
Mortar	Isotropic	21000	21000	21000	0.17
Horizontal Steel Layer	Isotropic	200000	200000	200000	0.30
Vertical Steel Layer	Orthotropic	200000	1000	1000	0.30
Wire Mesh Layer	Isotropic	138000	138000	138000	0.30

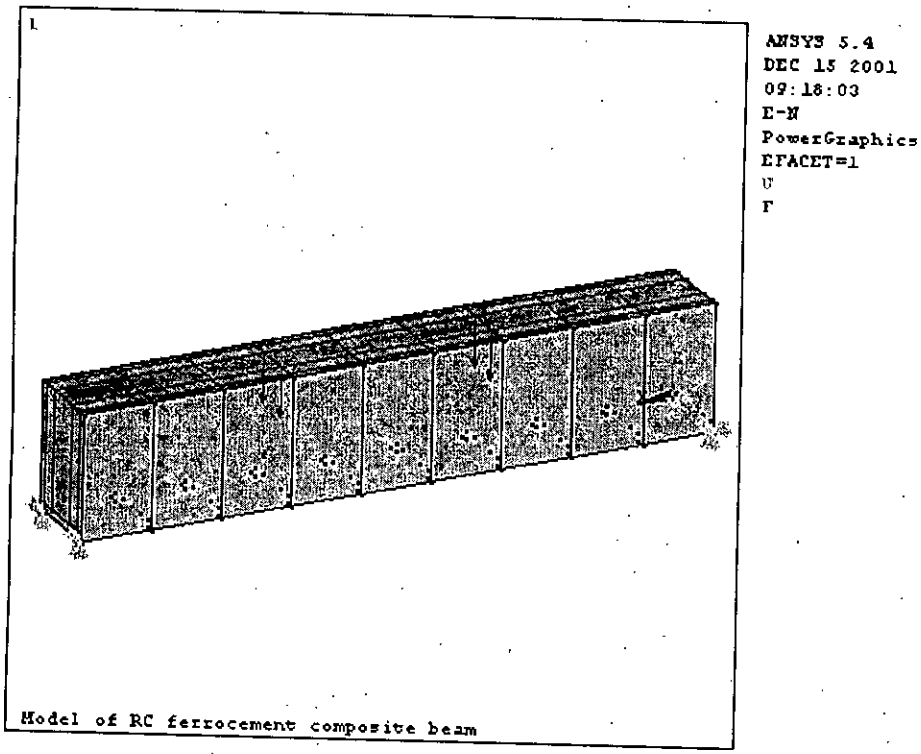

Fig. 4.5 3-D Model of the RC Ferrocement Composite Beam

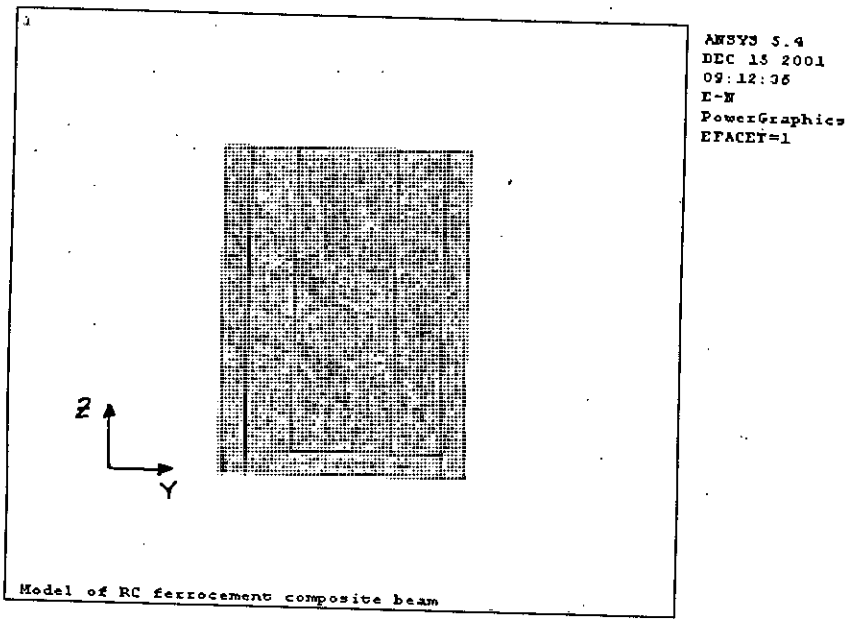

Fig.4.6 Cross-section of the Beam modeled in ANSYS

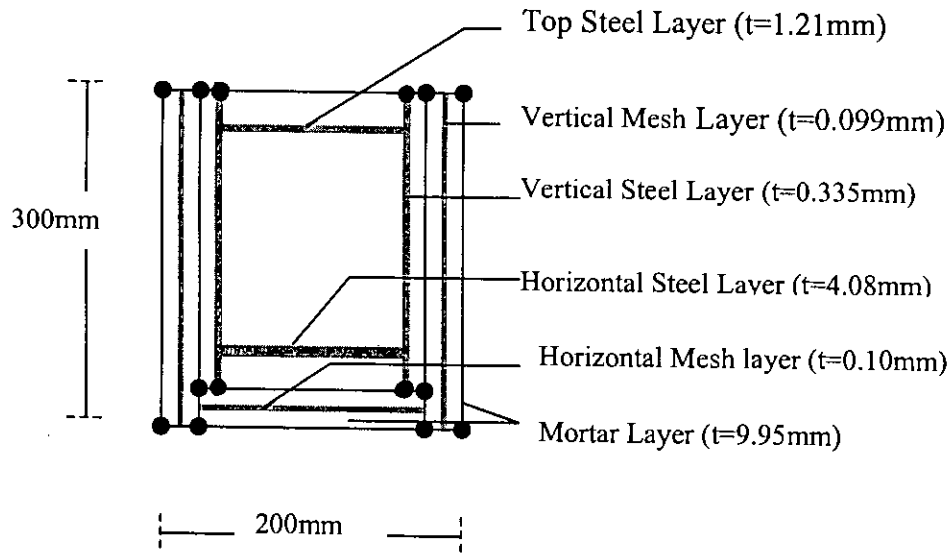

Fig.4.7 Thickness of the Equivalent Steel Layers for the Finite Element Model

After analysis comparison was made with respect to the cracking load and and corresponding deflection of the composite beam. The cracking load obtained form the analytical analysis is 66.56kN and that from finite element method is 73.20kN. The deflection corresponding to the cracking load from analytical and FEM analysis is 0.345 mm and 0.431mm respectively. The finite element model used in this study results in higher value of the cracking load and deflection of the beam than the analytical model by 10% and 20% respectively. The finite element model gives higher results compared to the analytical method for section analysis. This might be due to the idealization of the reinforcements by equivalent thickness of steel layers. This idealization might have increased the overall stiffness of reinfored concrete ferrocement composite system, than its actual stiftness value. This in turn resulted in higher cracking moments from the linear finite element analysis of the composite beam.

Chapter 5

RESULTS AND DISCUSSION

5.1 Introduction

Extensive experimental research works [Afsaruddin and Hoque,1998; Kadir et. al.,1997; Mays and Barnes,1994; Kaushik and Dubey,1994; Rosenthal and Bljuger,1985; Kaushik and Garg,1994] have been carried out to observe the cracking and ultimate behavior of reinforced concrete beams with ferrocement overlay. The theoretical results obtained from the analytical methods described in the previous chapter are presented here and compared with the experimental results available. This comparison will serve as verification for the validity of the proposed analytical model. The results of linear elastic finite element analysis using the package ANSYS, have also been compared with the results of the analytical model as well as with the experimental cracking moments to observe the performance of the layered finite element model for composite beams. The findings heve been discussed to highlight the important observations.

5.2 Experimental Investigations on Ferrocement-Reinforced Concrete Composite Beams

Although an extensive amount of research work has been conducted on the flexural behavior of reinforced concrete beams with ferrocement overlay, most of the published work is deficient in one or other data relating to the properties of materials used in the investigation and the reinforcement arrangements. This has seriously restricted the experimental data available for use in verifying the analytical method. Based on the availability of the basic data for the analysis of the composite beams, the works of Afsaruddin and Hoque,1998, Kadir et. al.,1997, Kaushik and Dubey,1994 and Rosenthal and Bljuger,1985, were selected for comparison with the analytical and finite element method.

The experimental works carried out by the above authors vary in the configuration of the reinforced concrete beams, ferrocement overlay, arrangement of reinforcement and the properties of the materials used. Therefore, first it is necessary to identify the sectional properties and the material properties for each experimental setup. Then, the cracking and the ultimate moments and corresponding deflections of the test beams will be calculated using the analytical method and hence compared with the actual experimental results. In case of any missing data assumptions are made based on judgment, to represent the actual condition as closely as possible.

5.2.1 Composite Beams of Afsaruddin and Hoque,1998

From the work of Afsaruddin and Hoque four composite beams designated as FB1, FB2, FB3 and FB4 are selected for comparison with the proposed analytical model. These beams are also modeled in ANSYS using the layered Solid 46 structural element and the cracking moment, determined from the finite element analysis is compared with the experimental cracking moments. The geometry and reinforcement details of these composite beams are shown in Fig.5.1.

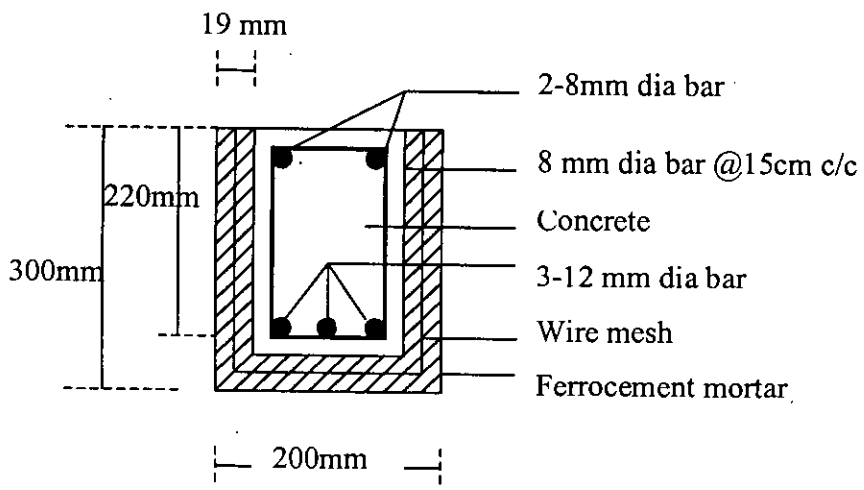

Fig.5.1 Cross-Section Details of Beam FB1(Afsaruddin and Hoque, 1998) (Actual size:204mm x 304mm)

For all the beams, 19 mm thick ferrocement layer was provided around the reinforced concrete section. 18 gauge woven square mesh, wire dia 1.2 mm with a mesh opening of 11.4mm x 11.4 mm, was provided in single layer in the ferrocement cover for all the composite beams. Sectional properties and material properties for the selected beams are given in Table 5.1 and 5.2 respectively. All the beams were tested under third point loading. Comparisons between the results are presented in Table 5.3.

Table 5.1 Sectional Properties of the Beams of Afsaruddin and Hoque

Beam Designation	Span	b	H	t_f	As	As_f	V_f
	m	mm	Mm	mm	sq. Mm	sq. mm.	%
FB1	1.52	224	304	19	340	19.8	1.03
FB2	1.52	226	304	19	314	19.8	1.03
FB3	1.52	162	254	19	226	19.8	1.03
FB4	1.52	164	254	19	236	19.8	1.03

Table 5.2 Material Properties of the Beams of Afsaruddin and Hoque

Beam Designation	f_y (MPa)	f_c' (MPa)	f_{ry} (MPa)	f_{rf} (MPa)
FB1	309	34.6	450	5.27
FB2	314	34.6	450	5.27
FB3	317	36.6	450	5.27
FB4	314	36.6	450	5.27

Table 5.3 Comparison of Results

Beam Designation	Cracking Moment (kN-m)					Ultimate Moment (kN-m)		
	Expt.	Analyt-ical	FEM	Expt/ Analy.	Expt./ FEM	Expt.	Analytical	Expt/ Analy.
FB1	19.7	19.75	21.7	1	0.91	30.4	27.88	1.09
FB2	16.6	19.86	21.9	0.84	0.76	49.8	31.03	1.6
FB3	12.5	9.9	10.92	1.26	1.14	29.1	15.26	1.91
FB4	11.5	10.03	11.05	1.15	1.04	32.2	15.35	2.1
Average				1.06	0.96	Average		1.67

From the table 5.3, it may be noted that both the analytical method and the finite element analysis estimate the cracking load (moment) equally well. The average value of the ratio of the experimental to analytical cracking moment is 1.06 and that of experimental to finite element results is 0.96. Thus, the correlation for both the analytical and numerical methods is found to be excellent for these beams. This implies that the analytical and FEM model performs quite well within the serviceability limit.

The finite element method adopted could not be used to estimate the ultimate moments for the composite beams. Hence, the experimental ultimate moments are compared with the analytical predictions only. From the table, it may be observed that the analytical solution grossly underestimated the ultimate moments in most cases and this is exhibited from the average ratio of 1.67 for the ultimate moments. In the case of ultimate limit state it is observed that the analytical method underestimates the strength of these beams. The effect of confining pressure imposed on the concrete core due to ferrocement overlay was not included in the analytical model. This may have partially contributed to under estimate the ultimate moment capacity.

5.2.2 Composite Beams of Kadir et. al., 1997

Among the sixteen composite beams tested by them eleven are selected for comparison with the analytical and FE method. Beams B1 through B5 of series 1 and B7 through B12 of test series 2 were analyzed by the analytical methods for comparison. Other beams B6 and B13 - B16 were excluded due to the absence of main rebar information.

The cross sectional properties and the material properties data for the beams used for the comparison purpose are presented in Table 5.4 and 5.5 respectively. All the beams were simply supported and were subjected to a two-point load test. The values of the cracking moment were not available in the paper only the ultimate moment and the failure load values were given. Therefore, the comparison (Table5.6) is made for the ultimate moment capacity of the composite beam sections. In this case, it is observed that the analytical solution

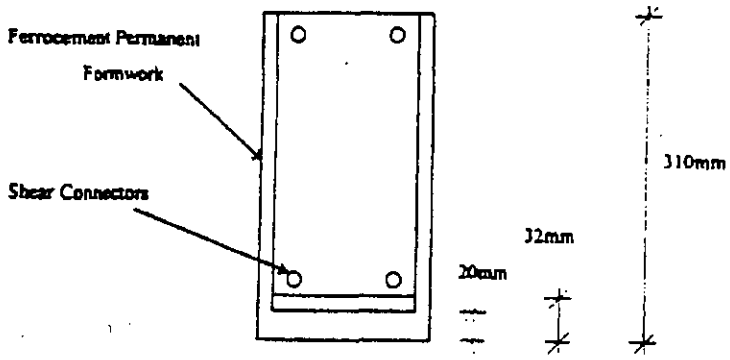

Fig.5.2 Details of Reinforced Concrete Beams with Ferrocement Permanent Formwork [Kadir, et. al.,1997]

underestimates the ultimate moment capacity compared to the experimental values. But, this time the predictions are fairly close for this series of beams. This can be seen from the average value of the ratio of 1.18 for experimental to analytical results for ultimate moments.

Table 5.4 Sectional Properties for the Composite Beams of Kadir et.al.

Beam Designation	Span	B	h	t_f	As	As_f	V_f
	m	mm	mm	mm	sq. mm	sq. mm.	%
B1	2.34	200	310	20	69	55	1.375
B2	2.34	200	310	20	141	55	1.375
B3	2.34	200	310	20	191	55	1.375
B4	2.34	200	310	20	245	55	1.375
B5	2.34	200	310	20	309	55	1.375
B7	2.34	200	310	20	90	55	1.375
B8	2.34	200	310	20	212	55	1.375
B9	2.34	200	310	20	250	55	1.375
B10	2.34	200	310	20	319	55	1.375
B11	2.34	200	310	20	402	55	1.375
B12	2.34	200	310	20	478	55	1.375

Table 5.5 Material Properties for the Composite Beams of Kadir et.al.

Beam Designation	f_y (MPa)	f_c' (MPa)	f_{ry} (MPa)	f_{rf} (MPa)
B1	415	27.6	450	6.03
B2	415	27.6	450	6.03
B3	415	27.6	450	6.03
B4	415	27.6	450	6.03
B5	415	27.6	450	6.03
B7	415	27.6	450	6.03
B8	415	27.6	450	6.03
B9	415	27.6	450	6.03
B10	415	27.6	450	6.03
B11	415	27.6	450	6.03
B12	415	27.6	450	6.03

Table 5.6 Comparison of Results

Beam Designation	Cracking Moment (kN-m)	Ultimate Moment (kN-m)		
	Analytical Results	Expt.	Analytical	Expt/Analy.
B1	18.78	21.50	18.19	1.18
B2	19.09	25.40	23.71	1.07
B3	19.23	31.20	27.43	1.14
B4	19.49	42.90	31.57	1.36
B5	19.78	42.90	36.44	1.18
B7	18.84	19.90	19.76	1.01
B8	19.41	25.40	26.91	0.94
B9	19.50	33.20	31.95	1.04
B10	19.81	50.70	37.18	1.36
B11	20.15	55.00	43.43	1.27
B12	20.34	70.20	49.04	1.43
Average				1.18

5.2.3 Composite Beams of Rosenthal and Bljuger, 1985

The experimental setup of the four rectangular composite beams studied by Rosenthal and Bljuger is shown in Fig.5.3 and the list of the material properties and cross-sectional dimensions are provided in Table 5.7 and 5.8. These beams are analyzed with the proposed analytical method and also with finite element method (FEM) and the results are compared with the experimental values (Table5.9). The experimental values of the ultimate strength of these beams are not available in the literature. Therefore the comparison was possible only in respect of the cracking moments of these beams. Again, it may be noticed that both analytical and FEM method estimates the cracking moment with excellent accuracy. The average ratio in both the cases is close to unity as can be seen in Table 5.9.

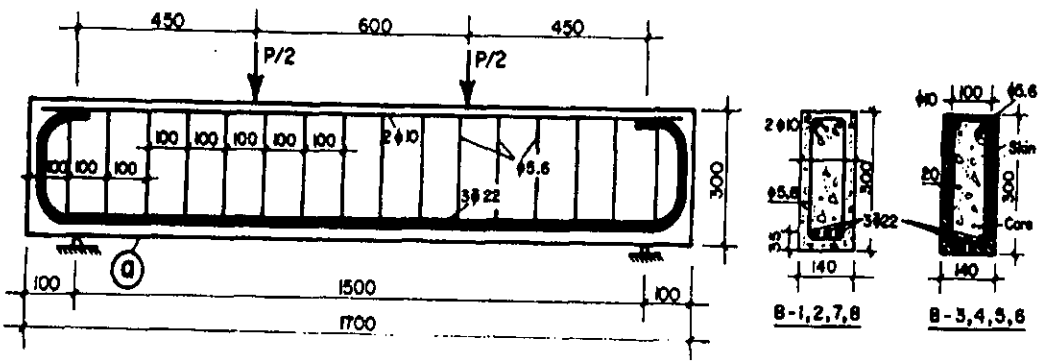

Fig.5.3 Composite Beam Specimens of Rosenthal and Bljuger,1985.

Table5.7 Sectional Properties for the Composite Beams of Rosenthal and Bljuger

Beam Designation	Span	b	H	t_f	As	As_f	V_f
	m	mm	mm	mm	sq. mm	sq. mm.	%
B-3	1.5	140	300	15	1140	20.37	1.94
B-4	1.5	140	300	15	1140	20.37	1.94
B-5	1.5	140	300	15	1140	19.66	1.44
B-6	1.5	140	300	15	1140	19.66	1.44

Table 5.8 Material Properties for the Composite Beams of Rosenthal and Bljuger

Beam Designation	f_y (MPa)	f_c' (MPa)	f_{ry} (MPa)	f_{rf} (MPa)
B-3	500	27	450	4.02
B-4	500	27	450	4.02
B-5	500	27	450	3.73
B-6	500	27	450	3.73

Table 5.9 Comparison of Results

Beam Designation	Cracking Moment (kN-m)					Ultimate Moment (kN-m)
	Expt.	Analytical	FEM	Expt/Analy.	Expt/FEM	Analytical
B-3	12.38	11.44	10.47	1.08	1.18	94.3
B-4	10.13	11.44	11.12	0.89	0.91	94.3
B-5	11.7	10.61	10.3	1.1	1.14	94.3
B-6	8.33	10.61	10.3	0.79	0.81	94.3
Average				0.97	1.00	

5.2.4 Composite Beams of Kaushik and Dubey, 1994

Reinforcement detailing and the cross-sectional dimensions of the composite beams selected from this study are shown in Fig.5.4 and the properties are listed in Table 5.10 and 5.11. The ferrocement jacket used was made with chicken wire mesh and typical section is shown in Fig. 5.5.

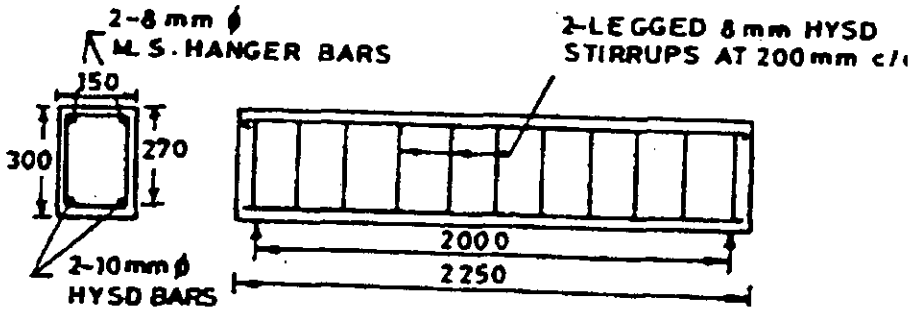

Fig.5.4 Reinforcement Details of R.C. Beams (Kaushik and Dubey, 1994)

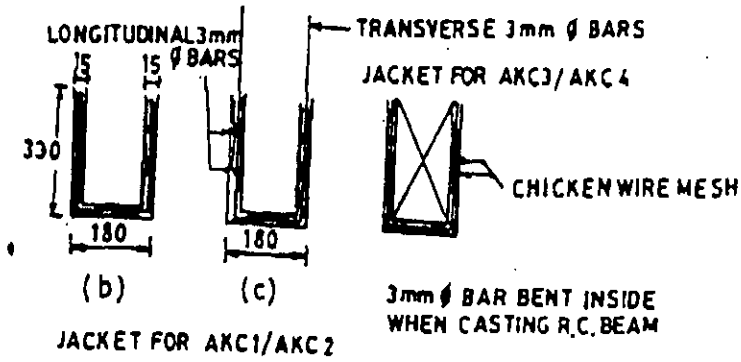

Fig.5.5 Reinforcement Details for Ferrocement Jackets (Kaushik and Dubey,1994)

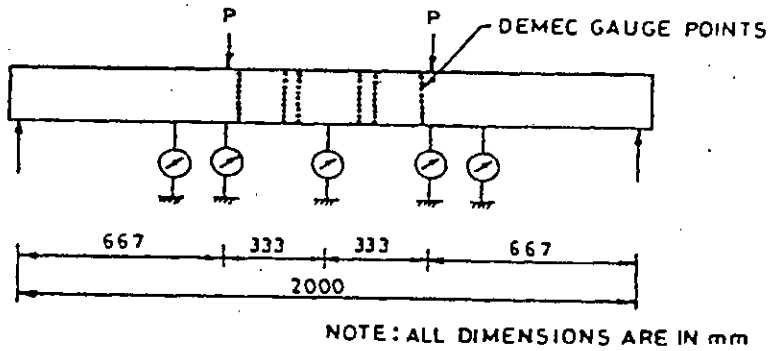

Fig.5.6 Typical Test Setup (Kaushik and Dubey,1994)

Table 5.10 Sectional Properties for the Beams of Kaushik and Dubey

Beam Designation	Span	b	h	t_f	As	As_f	V_f
	m	mm	mm	mm	sq. mm	sq. mm.	%
AKC1	2	180	330	30	157	12.15	0.27
AKC2	2	180	330	30	157	12.15	0.27
AKC3	2	180	330	30	157	12.15	0.27
AKC4	2	180	330	30	157	12.15	0.27

Table 5.11 Material Properties for the Beams of Kaushik and Dubey

Beam Designation	f_y (MPa)	f_c' (MPa)	f_{ry} (MPa)	f_{rf} (MPa)
AKC1	840	33.2	512	3.86
AKC2	840	33.2	512	3.86
AKC3	840	33.2	512	3.86
AKC4	840	33.2	512	3.86

Table 5.12 Comparison of Results

Beam Designation	Cracking Moment (kN-m)			Ultimate Moment (kN-m)		
	Expt.	Analytical	Expt/Analy.	Expt.	Analytical	Expt/Analy.
AKC1	8.3	10.7	0.78	28.23	24.57	1.15
AKC2	8.3	10.7	0.78	31.55	24.57	1.28
AKC3	9.96	10.7	0.93	28.23	24.57	1.15
AKC4	9.96	10.7	0.93	27.4	24.57	1.12
Average			0.86			1.18

The composite beams tested in this study differ only in the arrangement of the skeletal bars used in the ferrocement jacket. The other sectional properties and material properties of the test beams are identical. The effect of various arrangements of the skeletal bars in the jacket could not be modeled in the analytical solutions. For this reason the results of the analytical study are found to be identical for the four composite beams. And the average ratio of the experimental and analytical cracking and ultimate moments are found to be 0.86 and 1.18 respectively.

5.3 Conclusion

From the comparisons of the experimental results with that of analytical and finite element analysis solutions provided in the preceding articles, the following conclusions may be made.

(a) With respect to the cracking moment the analytical results were found to comply better with the experimental ones. The gross average ratio of the experimental and analytical values was found to be 0.96 (average of 1.06, 0.96, 0.86). This ascertains the validity of the idealizations and assumptions made in region I of the load-deflection response for the composite beam section.

(b) Usually the experimental results for cracking are found to be higher than the theoretical ones. But, in case of experimental results of Kaushik and Dubey,

1994, the values of the cracking moments were found to be lower than the theoretical values. They have used chicken mesh for construction of ferrocement jackets with differing skeletal bars. The effectiveness of chicken mesh compared to square mesh or expanded metal mesh is less and so the analytical model also underestimates the probable value.

(c) The linear finite element analysis results of the composite beams give satisfactory results for the cracking moments of the beams studied here.

(d) The experimental values of the ultimate moment capacity of the test beams were found to be always higher than the theoretical values. The over all average ratio of the experimental to analytical results was found to be 1.26. Twenty six percent overestimation is not too much considering the significant scatter of results observed in concrete construction. However, this might be due to the linear idealization of the load deflection response of the composite section and also due to the absence of the vertical ferrocement layer in the analytical model.

(e) In a ferrocement reinforced concrete composite beam the inner concrete core is confined with the outer U-shape ferrocement cover. The behavior of concrete is significantly improved when confined. Both the tensile and compressive strength of the confined concrete is much higher compared to its unconfined state and the failure of confined concrete occurs in a more ductile and gradual manner instead of failure in less ductile fashion as observed in its unconfined state. Therefore the confinement effect on the concrete core due to the ferrocement cover is responsible for the increased ultimate moment capacity of the composite section. The confinement effect was not considered in the analytical study. So, the analytical results are in general lower than the experimental values.

Chapter 6

EFFECT OF FERROCEMENT LAYER ON THE BEHAVIOR OF REINFORCED CONCRETE COMPOSITE BEAMS

6.1 Introduction

In this chapter the analytical response of typical composite beams with varying properties of ferrocement layer is studied. The proposed analytical method is used to observe the load deflection response of the composite beams and the finite element model is used to investigate the confinement effect of the outer ferrocement cover on the inner concrete core of the composite beams. As the ferrocement cover acts compositely with the reinforced concrete core, the behavior of the composite beam is influenced by the varying properties of ferrocement layer specially in the serviceability region. Two important parameters that have great influence on the crack resisting and the tensile properties of ferrocement are—volume fraction and the specific surface of the reinforcing mesh. These parameters again depend on the properties and number of the mesh layers used and the thickness of the ferrocement mortar. Thus, the behavior of the composite beam will greatly be affected by these two properties of ferrocement.

6.2 Load-Deflection Response of the Composite beams

To study the load-deflection response of the composite beam with varying properties of the ferrocement cover a typical reinforced concrete beam with ferrocement overlay is analyzed varying the number of mesh layers and thickness of the mortar in the outer cover. The analysis was done for single layer, double layer and triple layer wire mesh and in each of the cases the beam was again analysed by varying the thickness of the ferrocement cover. Therefor, the properties of the inner concrete core remains constant

convenience the resulting composite beams were designated as SB (with single layer wire mesh), DB (double layer wire mesh) and TB(tripple layer mesh). Again the SB beams were categorized as SB1, SB2, SB3, SB4, SB5, SB6 depending on the thickness of the ferrocement mortar used. DB and TB beams are also classified in the same manner. The range of variation of the thickness of the ferrocement cover is within 15mm to 30 mm. Square woven mesh with 1.2 mm wire dia and 11.4 mm×11.4 mm mesh opening are used in the ferrocement for all the beams studied. The cross sectional dimensions of these beams are summarized in Table 6.1 and 6.2. Table 6.1 mainly gives the basic properties of the ferrocement cover that distinguishes the beams from each other where as Table 6.2 provides the properties of the concrete core (that is kept constant for the resulting composite beams) and the additional parameters required for the estimation of the load-deflection response of these beams. Total 14 composite beams are analyzed using the analytical procedure described in chapter 3 for the estimation of the load-deflection response of these beams. The summary of the calculation of different terms in the three regions of the load-deflection response of these beams are provided in Table 6.3, 6.4 and 6.5. The resulting trilinear load-displacement curve of these composite beams are shown in Fig.6.1 through 6.7. The load-deflection response of the beams for fixed mesh layers like one, two and three layers with varying thickness of the ferrocement cover are shown in Fig. 6.1, 6.2 and 6.3. These figures indicate that the serviceability of the composite beams can be greatly improved by reducing the thickness of the ferrocement cover for a fixed mesh layer. It is also observed that the thickness of the mortar in ferrocement has a little impact on the ultimate behavior of the composite beam. The effect of increasing the number of mesh layers with constant mortar thickness can be observed from Fig.6.4 through Fig.6.7. Observing these load-deflection response for the composite beams analyzed, the effects of the number of mesh layer and the thickness of the ferrocement cover is investigated both in the serviceability and the ultimate limit state of these beams and are discussed below.

Table 6.1 Cross-sectional Properties of the Beams used in the Analysis

Beam Designation	Width b	Height h	Thickness of ferrocement layer t_f	t_f/h	No of mesh layers	Volume fraction V_f	Specific surface S_r	f_{rf}
	mm	mm	mm				1/mm	Mpa
SB1	200	300	15	0.050	1	0.0132	0.044	5.92
SB2	200	300	18	0.060	1	0.0110	0.037	5.49
SB3	200	300	20	0.067	1	0.0099	0.033	5.27
SB4	200	300	22	0.073	1	0.0090	0.030	5.09
SB5	200	300	25	0.083	1	0.0079	0.026	4.88
SB6	200	300	30	0.100	1	0.0066	0.022	4.62
DB2	200	300	18	0.060	2	0.0220	0.073	7.64
DB3	200	300	20	0.067	2	0.0198	0.066	7.21
DB4	200	300	22	0.073	2	0.0180	0.060	6.86
DB5	200	300	25	0.083	2	0.0159	0.053	6.45
DB6	200	300	30	0.100	2	0.0132	0.044	5.92
TB4	200	300	22	0.073	3	0.0270	0.090	8.62
TB5	200	300	25	0.083	3	0.0238	0.079	7.99
TB6	200	300	30	0.100	3	0.0198	0.066	7.21

Table 6.2 Additional Parameters used in Calculating the Load-Deflection Response of the Composite Beams

Beam Designation	b	h	t_f	cover for main bars	h_c	h_s	h_f	A_s	A_f	A_{fs}	E_f	m_1	m_2	m_3
	mm	mm	mm	mm	mm	mm	mm	sq mm	sq mm	sq mm	Mpa			
SB1	200	300	15	38	285	247	292.50	340	3000	19.80	22822	8	0.91	6
SB2	200	300	18	38	282	244	291.00	340	3600	19.80	22518	8	0.9	6
SB3	200	300	20	38	280	242	290.00	340	4000	19.80	22366	8	0.89	6
SB4	200	300	22	38	278	240	289.00	340	4400	19.80	22242	8	0.89	6
SB5	200	300	25	38	275	237	287.50	340	5000	19.75	22090	8	0.88	6
SB6	200	300	30	38	270	232	285.00	340	6000	19.80	21911	8	0.88	6
DB2	200	300	18	38	282	244	291.00	340	3600	39.60	24036	8	0.96	6
DB3	200	300	20	38	280	242	290.00	340	4000	39.60	23732	8	0.95	6
DB4	200	300	22	38	278	240	289.00	340	4400	39.60	23484	8	0.94	6
DB5	200	300	25	38	275	237	287.50	340	5000	39.75	23194	8	0.93	6
DB6	200	300	30	38	270	232	285.00	340	6000	39.60	22822	8	0.91	6
TB4	200	300	22	38	278	240	289.00	340	4400	59.40	24726	8	0.99	6
TB5	200	300	25	38	275	237	287.50	340	5000	59.50	24284	8	0.97	6
TB6	200	300	30	38	270	232	285.00	340	6000	59.40	23732	8	0.95	6

Table 6.3 Load-Displacements Calculations for Region I

Beam Designation	c	$(EI)_1$	I_1	M_1	P_1	k_1	δ_1
	mm	N-mm2	mm4	kN-m	kN	kN/m	mm
SB1	154	1.17E+13	4.69E+08	19.03	76.12	195930	0.389
SB2	153	1.17E+13	4.66E+08	17.41	69.64	194571	0.358
SB3	153	1.16E+13	4.64E+08	16.64	66.56	193687	0.344
SB4	153	1.15E+13	4.62E+08	16.00	64.00	192823	0.332
SB5	152	1.15E+13	4.59E+08	15.13	60.52	191560	0.316
SB6	152	1.14E+13	4.54E+08	14.17	56.68	189531	0.299
DB2	154	1.18E+13	4.70E+08	24.61	98.44	196295	0.501
DB3	154	1.17E+13	4.68E+08	23.12	92.48	195397	0.473
DB4	153	1.17E+13	4.66E+08	21.75	87.00	194511	0.447
DB5	153	1.16E+13	4.63E+08	20.31	81.24	193226	0.420
DB6	152	1.14E+13	4.58E+08	18.32	73.28	191145	0.383
TB4	154	1.18E+13	4.70E+08	27.75	111.00	196183	0.566
TB5	153	1.17E+13	4.67E+08	25.38	101.52	194872	0.521
TB6	153	1.15E+13	4.62E+08	22.65	90.60	192736	0.470

Table 6.4 Load-displacement Calculation for RegionII

Beam Designation	c	$(EI)_2$	M_2	P_2	k_2	Δ_2	δ_2
	mm	N-mm2	kN-m	kN	kN/m	mm	mm
SB1	71.05	2.84E+12	33.59	134.36	47365	1.230	1.618
SB2	70.56	2.76E+12	33.20	132.80	46144	1.369	1.727
SB3	70.23	2.72E+12	32.94	131.76	45339	1.438	1.782
SB4	69.90	2.67E+12	32.69	130.76	44542	1.499	1.831
SB5	69.40	2.60E+12	32.29	129.16	43356	1.583	1.899
SB6	68.57	2.48E+12	31.65	126.60	41431	1.688	1.987
DB2	72.08	2.90E+12	35.23	140.92	48349	0.879	1.380
DB3	71.75	2.85E+12	34.98	139.92	47531	0.998	1.471
DB4	71.42	2.80E+12	34.72	138.88	46721	1.110	1.558
DB5	70.94	2.73E+12	34.36	137.44	45536	1.234	1.655
DB6	70.10	2.61E+12	33.72	134.88	43557	1.414	1.798
TB4	72.90	2.93E+12	36.76	147.04	48872	0.737	1.303
TB5	72.41	2.85E+12	36.41	145.64	47662	0.926	1.447
TB6	71.58	2.73E+12	35.79	143.16	45656	1.151	1.621

Table 6.5 Load-Displacement Calculation for Region III

Beam Designation	c	$(EI)_3$	M_3	P_3	k_3	Δ_3	δ_3
	mm	mm^4	kN-m	kN	kN/m	mm	mm
SB1	31.97	2.03E+12	35.42	141.68	33975	0.215	1.833
SB2	31.97	1.98E+12	34.98	139.92	33084	0.215	1.942
SB3	31.97	1.95E+12	34.69	138.76	32497	0.215	1.997
SB4	31.97	1.91E+12	34.4	137.6	31915	0.214	2.045
SB5	31.97	1.86E+12	33.96	135.84	31045	0.215	2.114
SB6	31.97	1.78E+12	33.24	132.96	29642	0.215	2.202
DB2	33.87	2.13E+12	37.33	149.32	35520	0.236	1.616
DB3	33.87	2.09E+12	37.03	148.12	34914	0.235	1.706
DB4	33.87	2.06E+12	36.73	146.92	34314	0.234	1.792
DB5	33.88	2.00E+12	36.29	145.16	33444	0.231	1.886
DB6	33.87	1.91E+12	35.53	142.12	31970	0.226	2.024
TB4	35.77	2.19E+12	39.04	156.16	36631	0.249	1.552
TB5	35.78	2.14E+12	38.59	154.36	35726	0.244	1.691
TB6	35.77	2.05E+12	37.8	151.2	34216	0.235	1.856

6.3 Effect of Number of Mesh Layers

From the analytical response of the composite beams it is found that the resistance to cracking of the ferrocement RC composite beam increases to a great extent with the increasing number of mesh layers. Within the serviceability limit state the performance of the beam improves significantly just by doubling the mesh layer. This means that the cracking moment increases significantly with the increase in number of mesh layers as can be seen from Fig. 6.8. But, a little improvement is observed in the ultimate moment capacity of the beam with increase in number of mesh layers. This can be observed from the close spacing of the curves in Fig. 6.9. The other observations made from the analytical study performed on different series of beams are briefly stated as follows.

(a) Increase in the number of mesh layers within a constant thickness ferrocement layer will increase the volume fraction and the specific surface of the reinforcement which will result in high crack resisting capacity of the outer layer in the ferrocement reinforced concrete composite beam.

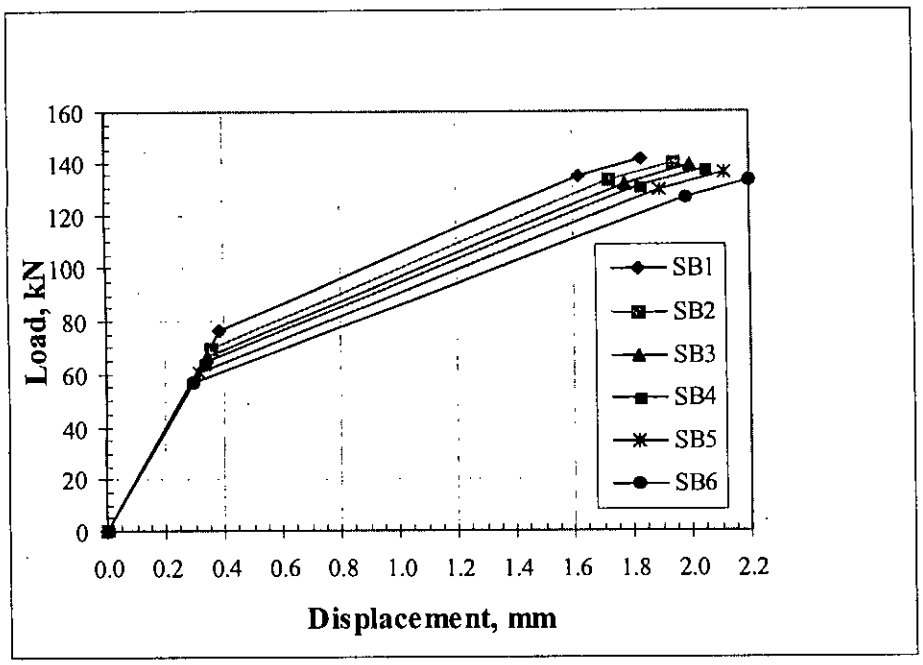

Fig.6.1 Load-Displacement Response for SB Series Beams

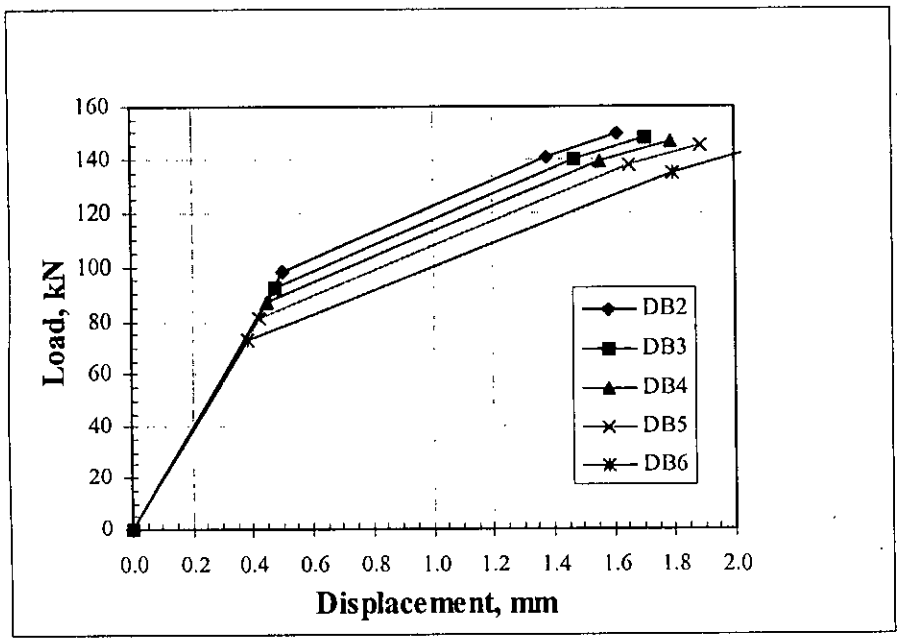

Fig.6.2 Load-Displacement Response for DB Series Beams

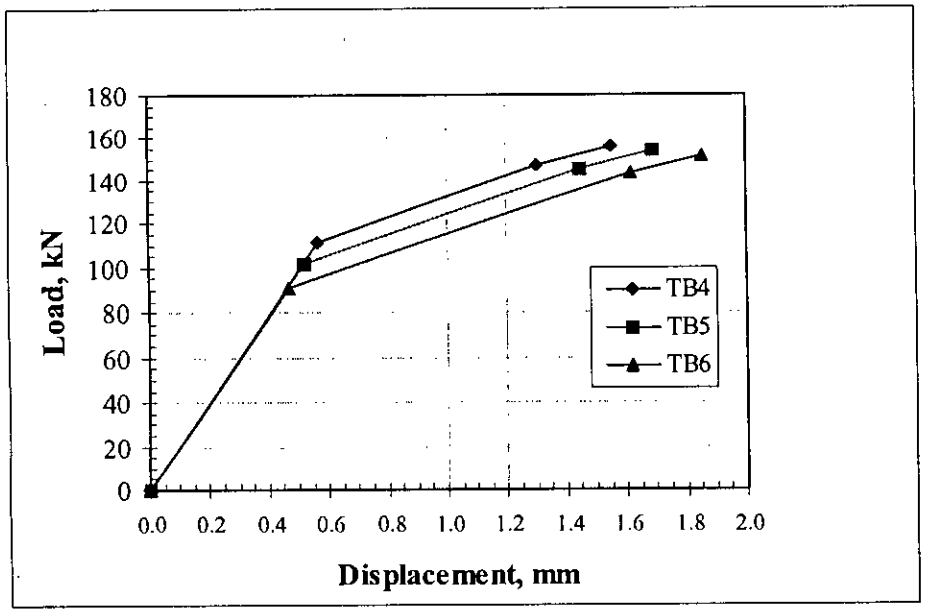

Fig.6.3 Load-Displacement Response for TB Series Beams

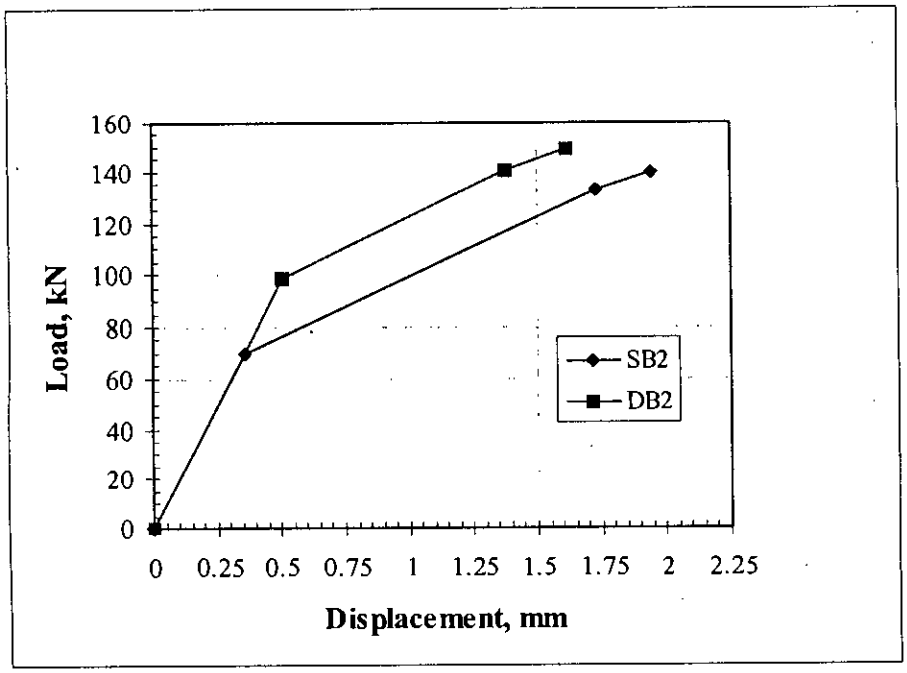

Fig.6.4 Load-Displacement Response with varying Number of Mesh Layers (t_f=18mm)

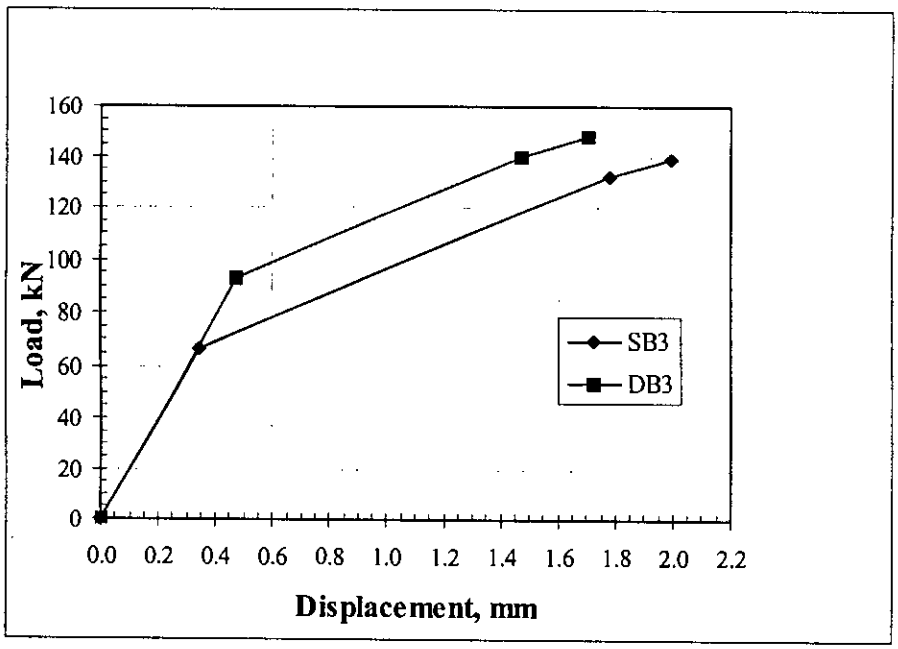

Fig.6.5 Load-Displacement Response with Varying Number of Mesh Layers (t_f = 20mm)

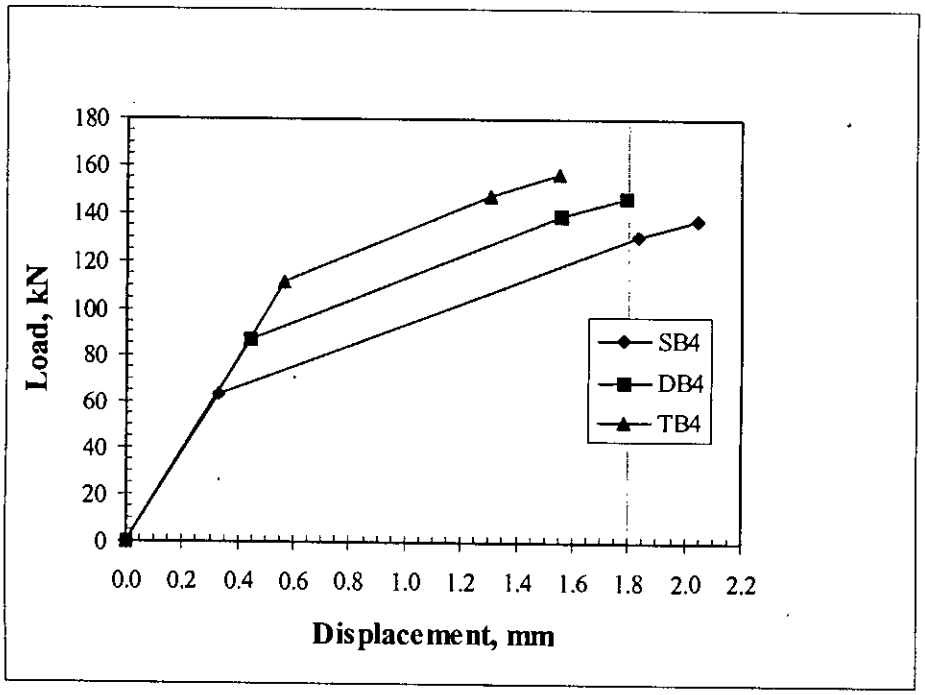

Fig.6.6 Load-Displacement Response with Varying Number of Mesh Layers (t_f = 22mm)

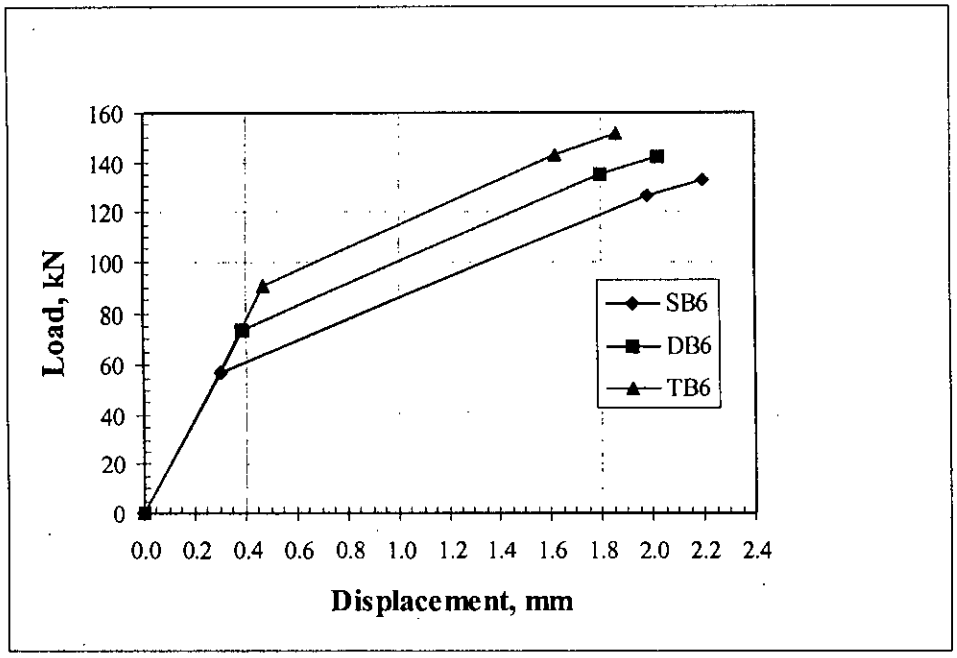

Fig.6.7 Load-Displacement Response with Varying Number of Mesh Layers (t_f = 30mm)

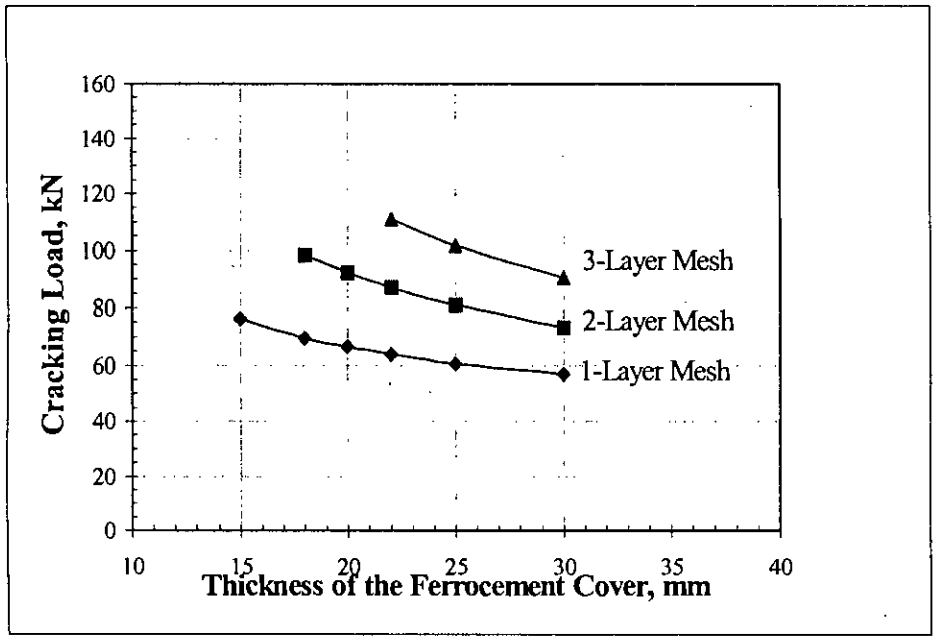

Fig.6.8 Cracking Load vs Thickness of Ferrocement cover for varying Mesh Layers

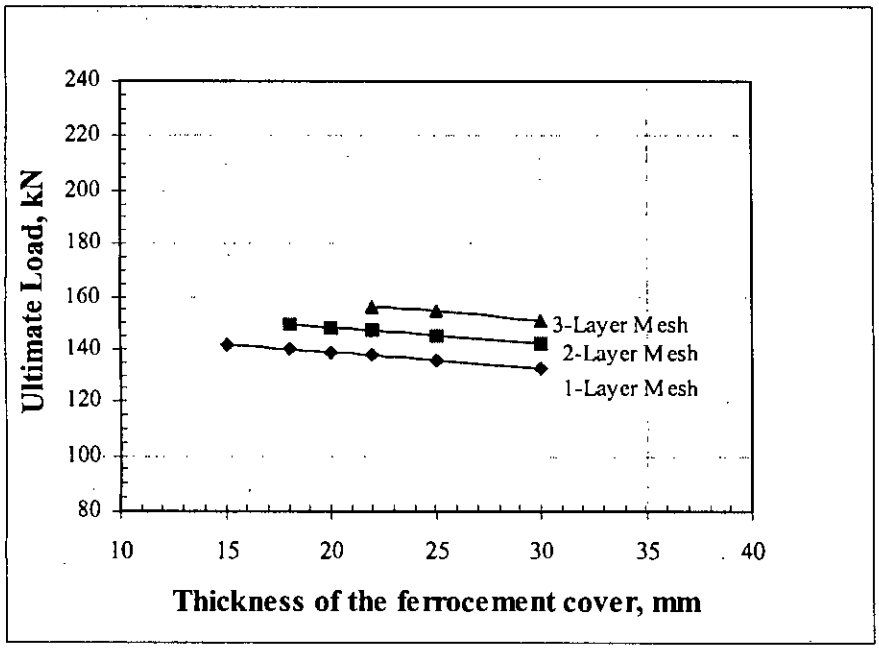

Fig.6.9 Ultimate Load vs Thickness of the Ferrocement for Varying Number of Mesh Layers

(b) The cracking moment and corresponding deflection of the beam is increased by 39% and 38% respectively by using double layer wire mesh with constant thickness of ferrocement layer (Table 6.6).

Table 6.6 Effect of Number of Mesh Layers on Moments and Deflections (t_f = 20 mm)

Parameter	SB3	DB3	%Variation
M_{cr}	16.64	23.12	39
δ_{cr}	0.344	0.473	38
M_2	32.94	34.98	6
δ_2	1.44	1.0	-30
M_3	34.69	37.03	7
δ_3	2.0	1.71	-14

(c) The effect of the number of mesh layers used has little impact on the ultimate moment capacity of the composite beams. The ultimate moment capacity of the beam in this study is found to be increased by only 7% (Table 6.6) by doubling the mesh reinforcement in the ferrocement layer.

(d) Another important observation is that the deflection in the postserviceability stage is reduced significantly about 15% by doubling the number of mesh layers. The rate of increase in the deflection with increasing load decreases with the increase in the percent of mesh reinforcement.

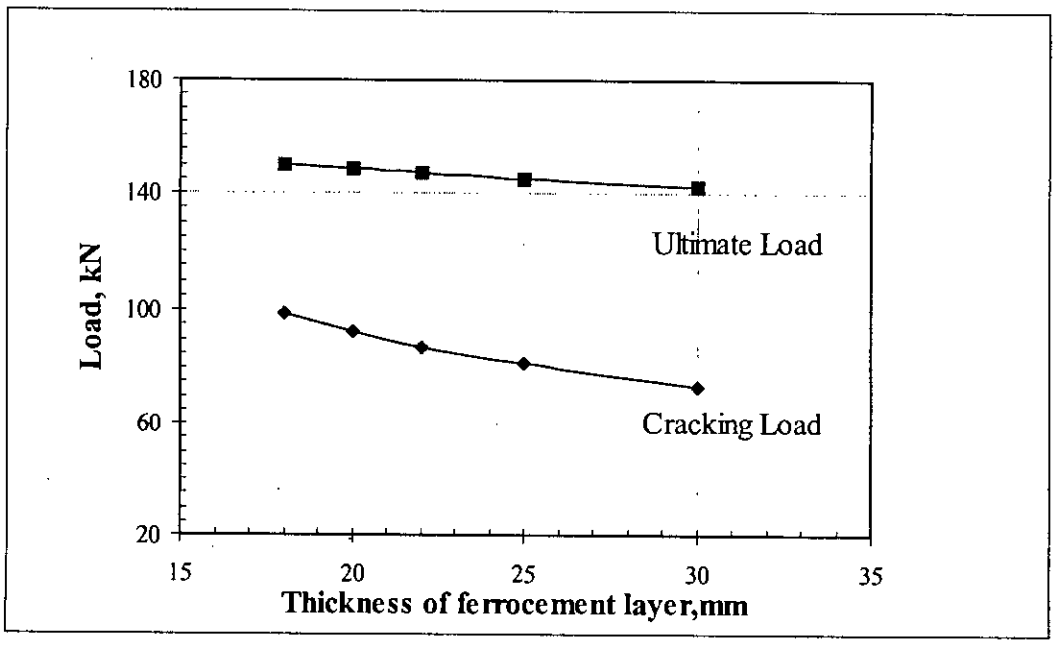

Fig.6.10 Variation of Ultimate and Cracking Load with Different Thickness of Ferrocement Layer

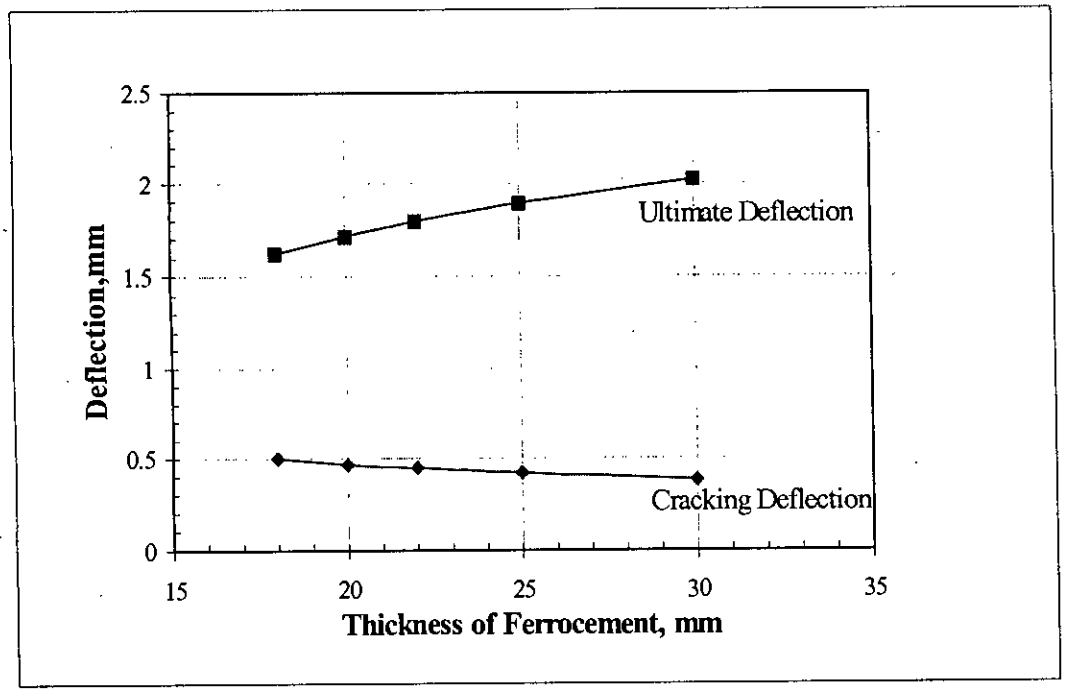

Fig.6.11 Variation of Deflection for Different Thickness of Ferrocement with Double Layer

6.4 Effect of the Thickness of the Ferrocement Layer

Observing the load-deflection response (Table 6.3 to 6.6), the effect of the thickness of ferrocement cover with double layer wire mesh on the load and deflection of the composite beams are shown in Fig.6.10 and 6.11 respectively and are discussed elaborately as follows.

(a) If the number of mesh layers and mesh properties remain constant then increase in the thickness of ferrocement mortar reduces the cracking moment of the beam. This occurs due to the reduction in the volume fraction and the specific surface of the reinforcing mesh.

(b) Thickness of the ferrocement cover has negligible impact on the ultimate load or moment capacity of the composite beam as can be observed from nearly horizontal ultimate load line in Fig. 6.10..

(c) From Fig.6.11 it is found that the thickness of the ferrocement cover has some influence on the ultimate deflection of the composite beam where as the effect on the cracking deflection is almost insignificant. The deflection values of the composite beam within the serviceability limit decreases with the increasing thickness. In the post serviceability region the deflection increases with the increasing thickness. After the formation of the crack, the thicker ferrocement cover greatly affects the serviceability of the beam and increases the deflection rapidly.

6.5 Confinement Effect of Ferrocement Overlay on Concrete

To investigate the confinement effect of the ferrocement cover on the reinforced concrete core one of the above beams say beam SB3 is analyzed by the finite element package ANSYS. The same beam without ferrocement cover is also analyzed by the finite element method and the resulting concrete compressive and tensile stresses are compared in both cases. The variation in the stresses for confined and unconfined state is shown in Table 6.7. It is observed that the resulting compressive stresses in concrete under flexure is reduced by 33% due to the confining pressure imposed on the concrete by the ferrocement overlay. Resulting tension in the composite beam is 40% lower than that of unconfined concrete beam.

Table 6.7 Confining Effect of Ferrocement Overlay on Concrete

Parameters	Confined State	Unconfined State	% Varriation
Maximum Tension (MPa)	4.18	6.23	33
Maximum Compression (MPa)	3.52	5.89	40

To observe the effect of the thickness of the ferrocement mortar and the number of reinforcing mesh on the confinement effect the composite beam is analysed by ANSYS with double layer mesh and for two different thickness 20 mm and 25 mm for the ferrocement layer. The resulting stresses are summarised in Table

Table 6.8 Effect of Ferrocement Properties on the Confining Effect

Thickness of Ferrocement, mm	Number of Mesh Layers	Maximum Compression (Mpa)	Maximum Tension (MPa)
20	1	4.18	3.52
	2	4.15	3.48
25	1	4.26	3.48
	2	4.23	3.44

Here it has been observed that the effect of the thickness of ferrocement and the number of mesh layers on the confinement of concrete is insignificant. In ferrocement forms for reinforced concrete beams, it is not feasible to increase the number of mesh layers more than three and the thickness of the ferrocement over 30 mm. The confinement effect is not significantly affected within this small range for these properties of ferrocement. But the stress resisting capacity of the reinforced concrete beam is greatly increased than its unconfined state. Due to lateral confinement the ductility of the beam is also increased which is very important for the structures in seismic region.

Chapter 7

CONCLUSIONS AND RECOMMENDATIONS

7.1 Conclusions

Flexural behavior of reinforced concrete beams with ferrocement overlay has been studied from two different approaches — an analytical method similar to reinforced concrete and finite element method. The load-deflection response of the composite beams with varying properties of ferrocement has been investigated using both these analytical approaches. Within the limited scope of the study, the following conclusions may be drawn.These conclusions are grouped under four sub-headings and are listed below.

Performance of the Analytical Model

(i) It is simple and direct and has been developed on the basic equilibrium requirements of a section as that of reinforced concrete.

(ii) The analytical model can trace the serviceability limit very well and the post serviceable response is also reasonably good.

(iii) The proposed model underestimates the ultimate strength. This may be due to the linear idealization of the stress-strain relationship of the constituent materials and the confinement effect of the ferrocement overlay. The ferrocement layers significantly restricts the growth and propagation of cracks in concrete even after the layer itself is cracked. This effect has not been included in the analytical model.

(iv) Tensile strength of the composite beam can be well predicted from the cracking strength of the outer ferrocement layer.

Load-Deflection Response of Composite Beams

(i) The serviceability range of the composite beams are significantly longer than the post serviceability range. This can be observed from the load-deflection response of the beams studied.

(ii) The load-displacement response is significantly affected by the properties of the ferrocement layer which in turn depend on the number of mesh layers and the thickness of the ferrocement mortar. However, it is the numbers of mesh layers that has more significant influence.

Performance of the Finite Element Model

(i) The layered finite element model in ANSYS used for analysis of the composite beams can be used confidently to estimate the cracking moments of the composite beams.

(ii) The layered model can be used to determine the confining pressure imposed on the concrete core by the outer ferrocement cover.

(iii) Confining effect of ferrocement on concrete is prominent and has a positive role to increase the cracking strength and serviceability range of composite beams. However, change in properties (mesh layers, thickness) of ferrocement have insignificant effect on confinement.

Design Suggestions

These suggestions are put forward with a view to attain maximum serviceability with minimum cost for the composite beams. The following suggestions are made as a guideline.

(i) Mortar thickness should be as minimum as possible say, between 20 and 30 mm.

(ii) Number of mesh layers should be one or at best two.

(iii) Mesh opening should be fairly close, say between 12 and 25 mm.

(iv) The confinement effect imposed on reinforced concrete beams by the ferrocement overlay must be taken into consideration in the design of such beams.

7.2 Recommendations

The following recommendations are made for future investigations.

(i) The analytical model may be extended to incorporate the analysis of doubly reinforced and flanged shape beams.

(ii) Further improvement to the analytical model can be brought by refining the load-displacement curve in the second region by varying the modulus of elasticity of concrete gradually.

(iii) Further analytical and experimental investigation is required to study the confinement effect of ferrocement and suggest analytical scheme to estimate it closely for design of ferrocement coated reinforced concrete composite beams.

(iv) Suitable nonlinear finite element model may be employed to trace the complete load-dsplacement response of composite beams with ferrocement overlay. A generalized model should be able to trace the behavior beyond cracking and serviceability limits and upto the ultimate failure stage.

(v) The effect of the dynamic loading on the behavior of the composite section may be investigated.

(vi) Effect of shear forces and bond on the flexural behavior of these composite beams may be investigated.

(vii) A continuous ferrocement overlay for the whole span length of the beam has been considered here. Further research work is suggested to study the effect of discontinuous or segmental ferrocement overlay on the behavior of composite beams.

REFERENCES

ACI Committee, 549, "State-of-the-Art-Report on Ferrocement", ACI Committee Report ACI 549R-93, November,1993, pp.1-12.

Afsaruddin, M. and Hoque, M.F., "Ferrocemnet as Permanent Formwork for Reinforced Concrete Beams", B.Sc. Engineering Thesis, Department of Civil Engineering, BUET, Dhaka, December 1998, pp24-30.

Anwar, A.W., Nimityongskul, P., Pama, R.P. and Robles-Austriaco, L., "Method of Rehabilitation of Structural Beam Elements using Ferrocement", Journal of Ferrocment, Vol.21, No.3, 1991, pp.229-234.

Collins, P.M. and Mitchell, D., "Prestressed Concrete Structures", Prentice Hall, Englewood Cliffs, New Jersey, 1991, pp.61-63, 79.

Johnston, C.D. and Mattar, S.G., "Ferrocement-Behavior in Tension and Compression", Journal of the Structural Engineering, ASCE, Vol.102, No.ST5, May., 1976, pp.875-889.

Johnston, Colin D., and Mowat, Dallas N., "Ferrocement--Material Behavior in Flexure", Proceedings, ASCE, V. 100, ST10, Oct. 1974, pp.2053-2096.

Kadir, M.R.A., Samad, A.A.A., Muda, Z.C. and Ali, A.A.A., "Flexural Behavior of Composite Beam with Ferrocement Permanent Formwork", Journal of Ferrocement, Vol.27, No.3, July 1997, pp.209-213.

Kaushik, S.K. and Dubey, A.K., "Performance Evaluation of RC Ferrocement Composite Beams", Proceedings of Fifth International Symposium on Ferrocement, UMIST, Manchester, September 1994, pp.241-255.

Lee, S.L., Raisinghani, M. and Pama, R.P., "Mechanical Properties of Ferrocement", FAO Seminar on the Design and Construction of Ferrocement Vessels, Oct.,1972.

Lin, T.Y. and Burns, N.H., "Design of Prestressed Concrete Structures", Third Edition, SI Version, John Wiley and Sons, New York, 1982, pp. 156-159.

Logan, D. And Shah, S.P., "Moment Capacity and Cracking Behavior of Ferrocement in Flexure", ACI Journal, Proceedings, Vol.70, No.12, Dec.1973, pp.799-804.

Lub, K.B. and Van Wanroij, M.C.G., "Strengthening of Reinforced Concrete Beams with Shortcrete Ferrocement", Proceedings of the third international Symposium on Ferrocement, University of Roorkee, Roorkee, India, Dec.8-10,1988, pp.477-484.

Mays, G.C. and Barnes R.A., "Ferrocement Permanent Formwork as Protection to Reinforced Concrete", Journals of Ferrocement, Vol.25, No. 4, October 1995, pp.331-345.

Naaman, A.E. and Shah, S.P., "Tensile Test of Ferrocement", ACI Journal, Vol.68, No.9, Sept.1971, pp.693-698.

Nanni, A. and Zollo, R.F., "Behavior of Ferrocement Reinforcement in Tension", ACI Materials Journal, Vol.84, No.4, July-Aug., 1987, pp.273-277.

Nawy, E.G., "Reinforced Concrete: A Fundamental Approach", Second Edition, Prentice Hall, Englewood Cliffs, New Jersey, 1990, pp.248-257.

Nilson, H., A., " Design of Concrete Structures", Twelfth Edition, The McGraw-Hill Companies, Inc., Newyork,1997, pp. 81-84.

Pama, R. P., "Ferrocement - An Overview", Keynote Lecture, Proceedings of Fifth International Symposium on Ferrocement, UMIST, Manchester, 6-9 September, 1994, pp.3-11.

Pama, R.P. and Paul B.K., "FERROCEMENT" , International Ferrocement Information Centre (IFIC), AIT, Bangkok, 1978, 34-40, 51-55.

Pama, R.P., "Research on Ferrocement - Global Perspective", Journal of Ferrocement, Vol.20, No.4, 1990, pp.385-410.

Pama, R.P., Sutharatanachaiyaporn, C., and Lee, S.L., "Rigidities and Strength of Ferrocement", First Australian Conference on Engineering Materials", The University of New South Wales, 1974.

Paramasivum, P., Mansur, M.A. and K.C.,Ong, "Flexural Behaviour of Lightweight Ferrocement Slabs", Journal of Ferrocement, Vol. 15, No. 1, January 1985, pp. 25-33.

Rao, A.K., " A Study of Behavior of Ferrocement in Direct Compression", Cement and Concrete, Oct.-Dec. 1969, pp.231-237.

Rao, C.B.K., and Rao, A.K., " Stress-Strain Curve in Axial Compression and Poisson's Ratio of Ferrocement", Journal of Ferrocement, Vol.16, No.2, April, 1986, pp.117-128.

Rosenthal, I and Bljuger, F., 1985, "Bending Behaviour of Ferrocement-Reinforced Concrete Composite", Journal of Ferrocement, Vol. 15, No.1, January, 1985, pp.15-23.

Surya Kumar, G.V. and Sharma, P.C., " An Investigation of the Ultimate and First Crack Strengths of Ferrocement in Flexure", Indian Concrete Journal, November 1976, pp. 335-340 & 344.

Walkus, B.R., "The Behavior of Ferrocement in Bending", Journal of Structural Engineering (Roorkee), V. 3, No. 3, Oct. 1975, pp.113-125.

APPENDIX

TYPICAL ANSYS DATA FILE

```
/prep7
antype,static
/title, Model of RC ferrocement composite beam

parres,,param.txt

!****************************************
!   MODEL GENERATION
!****************************************

C***Node Generation********************

n,1
n,2,,tf
n,3,,b-tf
n,4,,b
ngen,10,14,1,4,1,L/ne
n,5,,tf,tf
n,6,,(tf+tvc+tvs),tf
n,7,,(b-tf-tvc-tvs),tf
n,8,,b-tf,tf
ngen,10,14,5,8,1,L/ne
n,9,,0,h
n,10,,tf,h
n,11,,(tf+tvc+tvs),h
n,12,,(b-tf-tvc-tvs),h
n,13,,b-tf,h
n,14,,b,h
ngen,10,14,9,14,1,L/ne
!*****************************************


mp,ex,concrete,25000
mp,nuxy,concrete,.17
mp,ex,mortar,21000
mp,nuxy,mortar,.17
mp,ex,steel,200000
mp,nuxy,steel,.30
mp,ex,stirrup,200000
mp,ey,stirrup,1000
mp,ez,stirrup,1000
mp,prxy,stirrup,.30
mp,ex,wiremesh,138000
mp,nuxy,wiremesh,.30
```

```
C*****Define Elements and Real Constants***
et,1,solid46,,,,,2,4
keyopt,1,8,1
r,1,5
rmore
rmore,1,0,tbc,3,0,tbs
rmore,1,0,tmc,3,0,tts
rmore,1,0,ttc

r,2,2
rmore
rmore,1,0,tvc,4,0,tvs

r,3,3
rmore
rmore,2,0,(tf-tfs)/2,5,0,tfs
rmore,2,0,(tf-tfs)/2
!****************************************


C***Element Generation*******************

C***element 1-9 (middle horizontal layered elements of rc beam)
type,1
real,1
e,6,20,21,7,11,25,26,12
egen,ne,14,-1

C***element 10-18 (Vertical layered element of rc beam)
type,1
real,2
e,19,24,10,5,20,25,11,6
egen,ne,14,-1

C***element 19-27 (Vertical layered elements of rc beam)
type,1
real,2
e,22,27,13,8,21,26,12,7
egen,ne,14,-1

C***element 28-36 (horizontal ferrocement plate at the bottom)
type,1
real,3
e,2,16,17,3,5,19,22,8
egen,ne,14,-1

C***element 37-45 (Vertical ferrocement plate)
type,1
real,3
```

```
e,1,15,23,9,2,16,24,10
egen,ne,14,-1

C***element 46-54 (Vertical ferrocement plate)
type,1
real,3
e,3,17,27,13,4,18,28,14
egen,ne,14,-1

!*************************************************



C***Apply restraint*****************

d,1,all,,,4,1
d,1+ne*14,uz,,,4+ne*14,1,uy

!************************************


C***Apply Load**********************

f,11+ne*14/3,fz,-p/4,,12+ne*14/3,1
f,11+ne*14*2/3,fz,-p/4,,12+ne*14*2/3,1

!************************************

!END OF MODEL GENERATION


!**********************************
!   SOLUTION and RESULTS
!**********************************
finish
/solu
solve
finish
/post1
nsel,s,node,,64
/output,deflections.txt,,,append
prnsol,u,z
/output

esel,s,elem,,4
esel,a,elem,,13
esel,a,elem,,31
/output,stresses.txt,,,append
presol,s,x
/output
```

```
/output,strains.txt,,,append
presol,epto,x
/output
layer,2
/output,stressesL-2.txt,,,append
presol,s,x
/output
/output,strainsL-2.txt,,,append
presol,epto,x
/output
finish
/clear,nostart


!!END
```

TYPICAL ANSYS PARAMETER FILE

```
C***param.txt
C***Input for the cross sectional dimensions of the beam***
*set,h,300
*set,b,200
*set,L,1500

C***No. of finite elements***********
*set,lne,3
*set,ne,lne*3

C***Thickness of the ferrocement layer*****
*set,tf,20

C***thickness of the wire mesh layer in the ferrocement plate***
*set,tfs,.0992
!*set,tfs,.1984
!*set,tfs,.2976

C****Thickness of concrete and steel layer in the RC beam******
*set,tbs,4.08
*set,tts,1.21
*set,tvs,.335
*set,tbc,38.1
*set,tmc,198.51
*set,ttc,38.1
*set,tvc,38.1

C*****Material properties******
*set,concrete,1
*set,mortar,2
*set,steel,3
*set,stirrup,4
*set,wiremesh,5

C***Load Data*****
!*set,p,20000
!*set,p,40000
*set,p,50000
!*set,p,75000
!*set,p,90000
!*set,p,100000
!!END OF DATA
```